CHAPTER 1
INTRODUCTION

1.1 BACKGROUND OF STUDY

Solar drying goes back a long history. It traditionally began with drying by sun or better known as sun-drying. In this method, the product is exposed directly to sun rays allowing products to be dried by radiation from the sun. However, this method has disadvantages such as exposure of products to wind, rain, moist, dust, animals, insects and fungus growth. This process is also time consuming and requires large area.

From the concept of solar drying, solar dryers came up. The basic principle of a solar dryer is to pass hot, dry air heated by solar energy over products to be dried. Solar drying has been revealed to cost-effective and an efficient alternative to traditional and mechanical drying systems, especially in areas of good sunshine like Malaysia.

Various types of solar dryers have been designed to improve solar drying capabilities such as solar greenhouse dryers, solar cabinet dryers, forced convection dryers and many others. However, one major problem which exists with these solar dryers is their capability to dry products only with the existence of solar energy, enabling them to be operated only on hot days. This causes inconsistency in drying and a decrease in the production scale.

This project incorporates the use of the direct and indirect solar dryer with the biomass burner to sustain drying process even during night fall or cloudy weather. The biomass burner functions as an auxiliary heating system during times of low or zero intensity of solar radiation and thus, can be operated continuously, no matter with or without solar

energy. The actual model (FIGURE 1.1) has already been constructed by a past Final Year Student. The author's job is to produce the simulation model and to conduct experiments on the actual solar dryer.

FIGURE 1.1: Hybrid Solar Dryer with Biomass Integration

Computer Fluid Dynamics (CFD) technique is used to simulate the model in order to analyze the performance of the dryer and the fluid flow in the dryer. Modeling is done to compare the simulation results by CFD technique with the analytical results from experiments and data collection.

1.2 PROBLEM STATEMENT

One of the oldest uses of solar energy since the dawn of civilization has been drying and preservation of agricultural products. Since this method is simple and utilized in most countries, its acceptance does not create any problem. Although solar drying is accepted by many, there still exist some problems concerning solar drying for example, non-continuous input of solar due to nightfall.

1.2.1 Problem Identification

Several issues related to current solar drying methods are described as below:

- Sun-drying is the conventional drying method used since the olden days. Food is exposed directly to the sun and therefore is open to dust, rain, animals, and insects. Nutrient deficiency also occurs due to direct radiation from the sun causing food to lose certain vitamins.

- Mechanized dryers use electricity or fuel to operate the system thus causing the system to be rather costly.

- Current solar dryers can only operate when there is solar radiation. They cannot function during times of low solar radiation or during nightfall. Therefore, they cannot be operated continuously causing low production rate.

1.2.2 Significance of Project

Drying is an excellent way to preserve food and solar food dryers are an appropriate food preservation technology. Proper usage of solar energy produces food of better quality and provides reduction in drying time compared to open sun drying. Drying is also important for drying of wastes, timber, etc. Besides, solar drying processes are cost-effective and environmental friendly. By incorporating the use of a biomass burner as a backup system, products can also be dried during cloudy weathers and also at night. Thus, drying can be done continuously and this consequently increases production. With the application of numerical method using FLUENT, simulations can be conducted to represent the real life scenario of the solar dryer. Hence, modifications on the simulated model can be done to obtain the optimum design for the solar dryer without cost wastage in the case of modification made on the actual model.

1.3 OBJECTIVES AND SCOPE OF STUDY

1.3.1 Objectives

- Simulation of a hybrid solar dryer model based on CFD method using FLUENT and GAMBIT software.
- Analyze the thermo fluid process in the dryer based on heated air by solar drying and by biomass energy.
- Conduct series of measurements on the experimental solar dryer model and compare with simulations from CFD method.

1.3.2 Scope of Study

This project is to be completed based on the scope of study as listed below:

(a) Research and study on the mechanism of the solar drying system.
(b) Research on the hybrid dryer.
(c) Model and simulate the solar cum biomass dryer design using FLUENT and GAMBIT.
(d) Conduct experiments on the real model and compare with simulation results from FLUENT.
(e) Justify the overall performance of the solar dryer system.

CHAPTER 2
LITERATURE REVIEW

Agriculture and other products have been dried in sun since thousands of years back. The purpose is either to preserve them for later use as in the case of food; or as an integral part of production process as with timber and oil palm wastes.

A great deal of study over the past few decades has demonstrated that agricultural products can be satisfactorily dehydrated using solar energy. Major concerns regarding these solar dryers are their non-reliability due to their operations which depends largely on weather conditions and their low-productivity due to production only when there is solar energy. The hybrid dryers are the solvers of this issue and many studies have been conducted in order to develop hybrid dryers which are efficient, low-cost and reliable.

Simulation is a very important process in engineering systems, especially for solar systems. Simulation models are needed to study the result of the drying process and to work on improvements and modifications on the solar dryer model. This literature review presents a research on solar dryers in the market and a more precise study on solar hybrid dryer studies that has been conducted in the past.

2.1 HOW SOLAR DRYERS WORK

Drying is a dual process of (a) heat transfer to product from heating source and (b) mass transfer of moisture from interior of product to its surface and consecutively to the surrounding air [1]. In solar drying, air flow is generated either by forced or natural convection.

Solar dryers use the sun's radiation to heat the air that flows over the food. Humidity of the air decreases as it is heated and is capable to hold more moisture. The heated, warm, dry air is then able to carry away moisture evaporated from the product [2].

For effective drying, air should be hot, dry and moving. The lower the humidity, the drier the air. Dry air has the capacity to pick up water vapor from the products and remove it. Wet air becomes saturated very quickly and cannot pick up additional water vapor from the products [3].

2.2 CLASSIFICATIONS OF SOLAR DRYERS

Solar dryers fall into two broad categories which are active and passive. These two categories can be further divided into direct, indirect and mixed models. A direct dryer is one in which the product is directly exposed to the sun's rays. In an indirect dryer, the sun's rays do not shine directly on the product to be dried [4].

2.2.1 Direct Solar Dryers

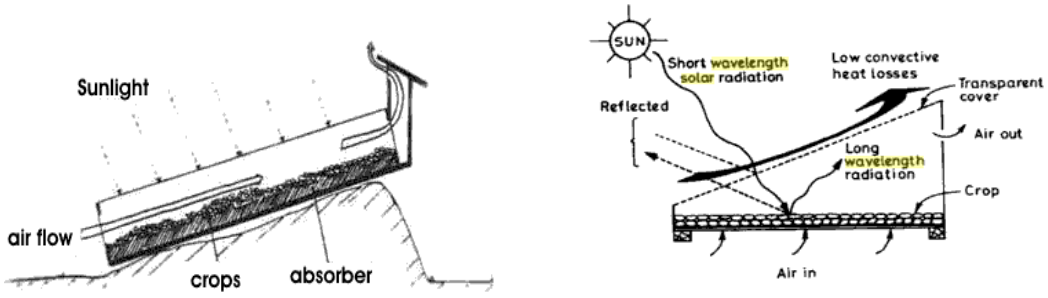

(a) **(b)**

FIGURE 2.1: **(a)** Direct Solar Dryer [5], **(b)** Concept of Direct Solar Dryer [6]

In Direct Solar Dryers, products placed in a transparent enclosure of glass or plastic absorbs solar radiation directly from the sun. Sun radiation penetrates through glazing due to short wavelength. As radiation energy penetrates through the glazing, it changes from short wavelength to long wavelength due to lost in energy. This causes 'greenhouse effect' where heat removes moisture from product.

2.2.2 Indirect Solar Dryers

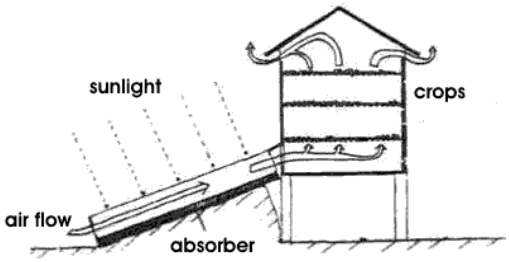

FIGURE 2.2: Indirect Solar Dryer [5]

In Indirect Solar Dryers, solar radiation does not act directly on product. This method can minimize discoloration and nutrient loss. A separate solar collector absorbs radiation and converts it into thermal energy. Thermal energy heats up the flowing air which is then ducted to the drying chamber to dehydrate the product. Warm, moist air evaporated from solar drying process is released out through the chimney.

2.2.3 Mixed-mode solar dryers

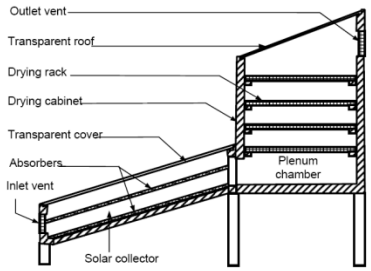

FIGURE 2.3: Mixed mode Solar Dryer [7]

Mixed-mode Solar Dryers absorbs solar radiation by two ways: a separate solar collector and also through the transparent walls and roof. Radiation is absorbed by a separate solar collector and hot air is ducted up from separate solar collector to the drying chamber. Radiation also penetrates through glazing and heat is trapped in drying chamber.

2.3 HYBRID BIOMASS SOLAR DRYER

In hybrid biomass solar dryers, a biomass-heat exchanger is incorporated in the solar drying system in order to reduce its dependence on solar radiation. This is to enable continuation of the drying process even when at night or during cloudy weather [8], [9]. Biomass (especially wood), is a dominant source of energy. This resource if used competently can be used as a back-up source for solar energy [9].

A heat exchanger is integrated in the design so that flue gas from the biomass burner would not mix with the drying air. This is to avoid contamination of food products by smoke, soot and ash [8], [9].

2.4 DRYING METHODS OF BIOMASS INTEGRATED SOLAR DRYERS

Several methods to improve solar drying have been investigated. One of the investigated methods to improve solar drying is by using a solar hybrid dryer. The hybrid dryer is used as a normal solar dryer during the day and the biomass stove was designed mainly to sustain the solar operation of the dryer during cloudy weather and at night [11], [12], [13], [14]. Biomass source, such as agriculture residue and wood has found to be the most suitable energy source for drying purpose due to ease of access [14], [15].

During periods of low or zero solar radiation, biomass burner is used for back up heating [11], [12], [13]. The combustion gases heat up the box surface, which in turn warm the air as it moves over the outer surface. The warm air rises up into the drying chamber, evaporating and picking up moisture from the produce as it passes through the trays, and then escapes through the top vents [12], [13].

Various analyses have been implemented to study the effectiveness of the solar hybrid dryer. Several analyses are described in the following sections.

2.4.1 Hybrid Solar Dryer with Biomass Integration

This project was done by a previous Final Year Project (FYP) student. A mixed-mode hybrid solar dryer with biomass integration has been designed, constructed and evaluated. This project aims to carry out experimental investigations using solar as main input to the dryer and biomass burner as an auxiliary source of energy. Major components of the fabricated dryer are the biomass, solar collector and drying chamber [10].

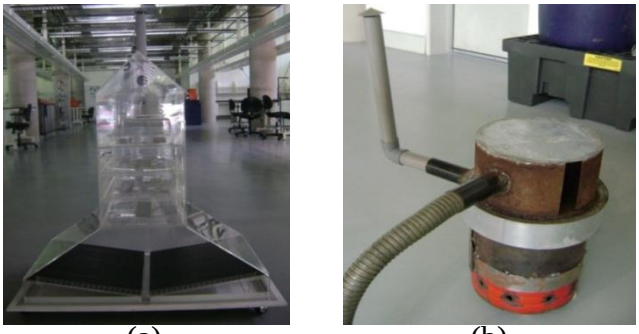

(a) (b)

FIGURE 2.4 (a): Solar hybrid dryer [10], **(b)**: Biomass burner [10]

The dryer was tested using three operation modes which are solar drying mode, biomass drying mode and combined drying mode, by drying 200g of empty fruit bunch (EFB). Results show that combination mode by drying with solar and biomass simultaneously, is the most effective. Moisture content reduction of almost 50% is obtained within 2 hours [10].

2.4.2 Solar-Biomass Hybrid Tunnel Dryer

A solar-biomass hybrid tunnel dryer has been designed and fabricated. A biomass-stove heat exchanger chimney using briquetted rice husks as fuel complements the solar tunnel dryer. This solar-biomass hybrid dryer which consists of a flat plate solar collector and a drying tunnel fabricated as a single unit. The 'tubes' of heat exchanger were connected to a biomass stove at one end and a chimney at the other. Heating on food is indirect so that flue gas from biomass stove and drying air would not be mixed. This is to avoid contamination by smoke, soot and ash of flue gas [11].

FIGURE 2.5: Solar-biomass Hybrid Tunnel Dryer [11]

Experiments have been conducted by drying chilies and mushrooms. Based on tests conducted for chilli, 19.5 kg of ripe, fresh chilli, had reduction of moisture content from 76% to 6.6% within 12 hours and for tests on 21 kg of mushrooms, moisture content reduced from 91.4% to 9.8% within 12 hours of drying [11].

2.4.3 Integral type Natural Convection Solar Dryer Coupled with Biomass Stove

An integral type natural convection solar drier has been fabricated and coupled with a biomass stove to test its performance by drying *Zingiber officinale* (ginger), *Curcuma longa l.* (turmeric) and *Tinospora cordifolia* (guduchi) during the summer climate in Delhi [12].

FIGURE 2.6: Natural Convection Solar Dryer coupled with Biomass Stove [12]

It was found that, during the load test for ginger, 18 kg of fresh product with an initial moisture content of 319.74(db) % was dried to a final moisture content of 11.8(db) % within 33 hours. Similarly, moisture content of turmeric and guduchi were reduced from

358.96(db) % to 8.8(db) % and 257.45(db) % to 9.67(db) % during 36 and 48 hours of drying, respectively. It was also found that drying time has been reduced to 54–60% and 83–84% in solar-biomass hybrid drier in comparison to 'only solar' and open sun drying operations [12].

2.4.4 Direct Natural Convection Solar cum Biomass Dryer

A direct type natural convection solar cum biomass dryer was developed. This system consists of single glazed solar cabinet dryer mounted on a biomass chamber. Drying parameters were observed at five different points and samples were weighed at different time intervals [13].

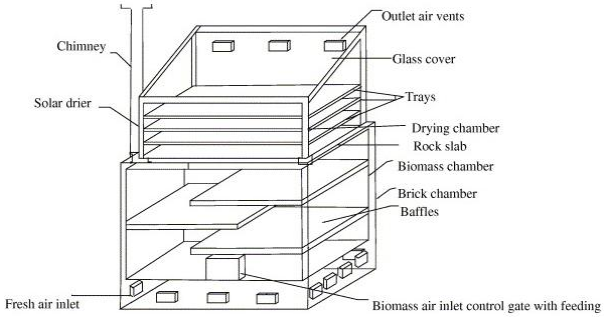

FIGURE 2.7: Direct type natural convection solar cum biomass dryer [13]

Performance of the dryer is tested by drying turmeric rhizomes. The system is capable of generating continuous flow of hot air at 55 - 60°C. Drying time for turmeric had a reduction time of 86% compared to sun drying and its efficiency was 28.57% [13].

2.4.5 Hybrid Solar Biomass Cabinet Dryer

A biomass stove has been installed at one side of the drying chamber of the basic solar collector, in adjacent to the collector system to work as a hybrid dryer. Hot flue gas from the stove is passed through the heat exchanger, installed at the bottom of the drying chamber. The heat exchanger transfers its heat to the ambient air coming through the solar collector into the drying chamber. After having passed through the heat exchanger, flue gas exists through the outlet, installed at another side of the drying

chamber. Heated ambient air enters into the drying chamber and then passes through the products to be dried. Hot and moist air from the drying chamber exits through the chimney placed at the top of the chamber [14].

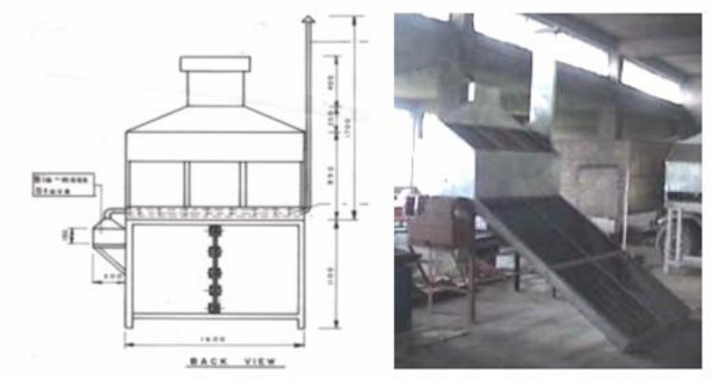

FIGURE 2.8: Basic solar collector with one side of drying chamber attached to biomass stove [14]

From the performance evaluation of a hybrid solar biomass cabinet dryer in drying cauliflower, the efficiency was revealed to be 16.32% [14].

2.4.6 Rotary Solar Hybrid Dryer

A rotary solar hybrid dryer (FIGURE 2.9) has been designed and developed for copra drying. The drying chamber (FIGURE 2.10) was designed to rotate manually around the axis of heat chamber. The drying chamber was designed to have a cylindrical shape. This is to facilitate rotation and mixing for uniform drying. The furnace was fired with paddy husks at different feeding rates [15].

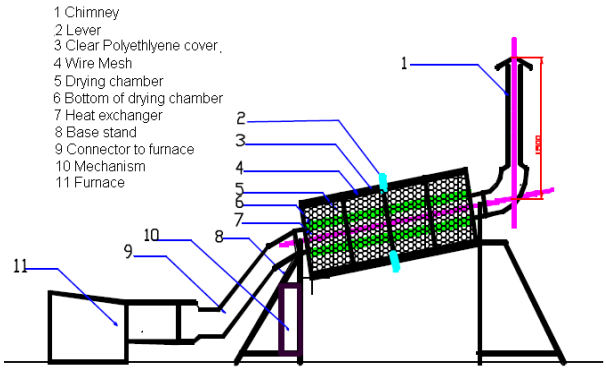

FIGURE 2.9: Complete system of the rotary solar hybrid dryer [15]

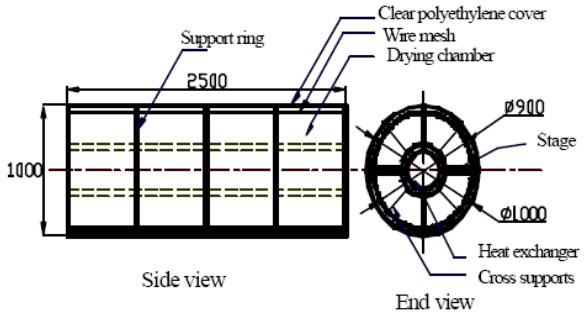

FIGURE 2.10: Drying chamber of rotary solar hybrid dryer [15]

The average drying chamber temperatures at the husk feeding rates of 3 kg/h, 5 kg/h and 10 kg/h were 43°C, 53°C and 62°C and furnace efficiencies were 43%, 48% and 70% respectively. Furnace efficiency increased with increasing husk feeding rates. White copra was dried to a moisture content of 7%. About 70 hours of continuous drying was needed to complete the drying process at overall thermal efficiency of 10% [15].

2.5 SIMULATION ANALYSIS

Author conducted research on journals and previous works concerning simulations of solar dryers. However, the journals obtained were not directly related to simulations on solar dryers and as a result, not presented in this literature review. Therefore, entire works on this project were based on numerous tutorials in FLUENT manual, discussions, brain-storming and also based on trials and practices.

2.6 CONCLUSION BASED ON LITERATURE REVIEW AND RESEARCH

The mixed-mode hybrid solar dryer with biomass integration design made by the previous final year student is different compared to other designs from literature reviews. Hence, CFD analysis is necessary to ensure the workability and effectiveness of this design.

CHAPTER 3
METHODOLOGY

3.1 TECHNIQUE OF ANALYSIS

Two analysis techniques have been adopted, experimental and numerical. This project is conducted by modeling the design based on CFD method using FLUENT. The modeling is done to investigate the fluid flow through the solar dryer and to compare the simulation results with the data collection results obtained based on experiments conducted on the established model. This comparison is made to improve on any problems that occur with the solar dryer model and to ensure workability and efficiency of the solar dryer.

3.1.1 Process operation of the solar dryer

Understanding the process operation of the solar dryer is essential for the author in order to design and simulate the correct model. Besides, this understanding also guides the author when conducting experimentation on the model.

The solar dryer utilizes solar energy from the sun during the day. Solar radiation falls unto the dryer and is absorbed by the absorber causing an increase in temperature inside the solar dryer. Thus, there is temperature difference between the inside and outside of the solar dryer. Heated air inside the cabinet picks up moisture from the products and is released as hot, moist air through the chimney. This reduces the pressure inside the cabinet and ambient air is drawn into the dryer through the inlet holes.

When there is no solar energy, this dryer incorporates the use of the biomass burner to dry products. Combustion gases from the solar burner heats up the biomass chamber by direct flue. However, in the case of food products, flue gas passes through a heat exchanger and warms the air moving across its surface. The warmed air rises into the drying chamber of the solar dryer, passes through the trays and picks up moisture from the products. The warm, moist air then escapes through the chimney.

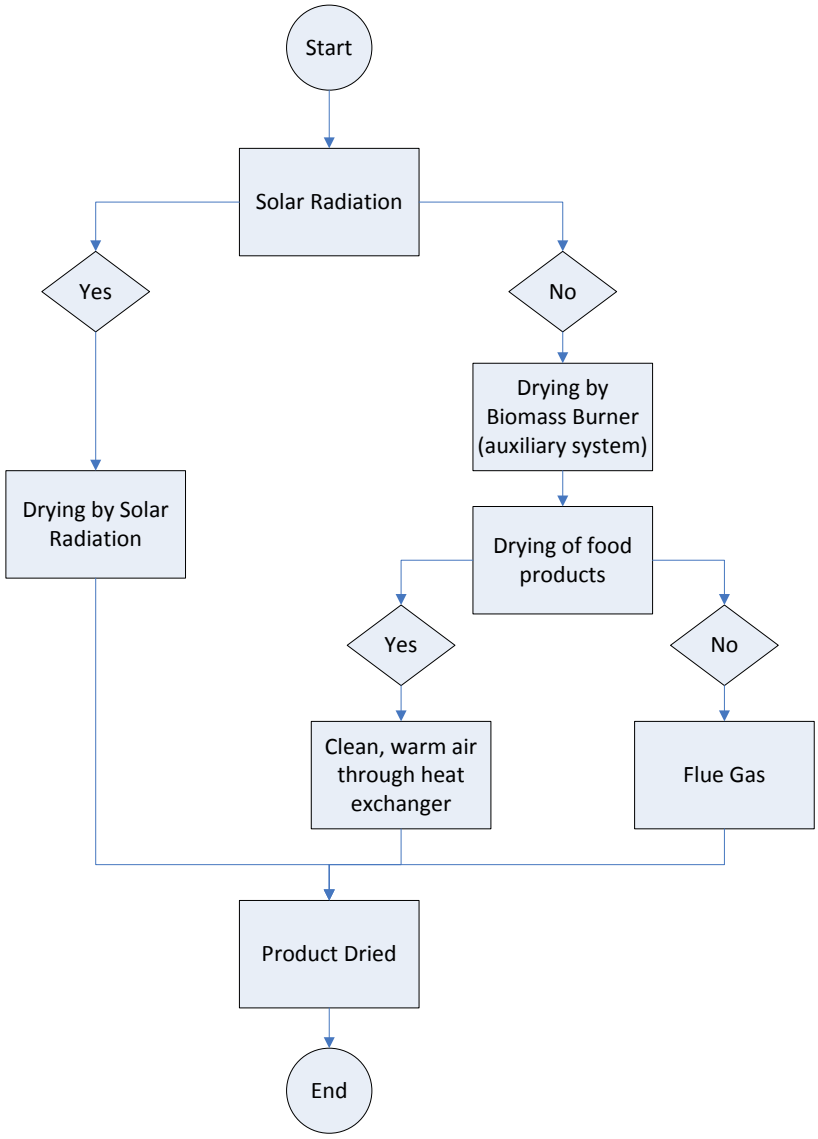

FIGURE 3.1: Flowchart of drying process of the multipurpose solar dryer

3.2 PROJECT ACTIVITIES

Project begins with a thorough study on solar dryers. Model is then constructed based on dimensions obtained the actual solar dryer assembled by a past FYP student. Parameters such as velocity input and temperature of absorber is set as input parameters in FLUENT to run the simulation. Experiments are also conducted on the actual model and results obtain are compared with simulation results.

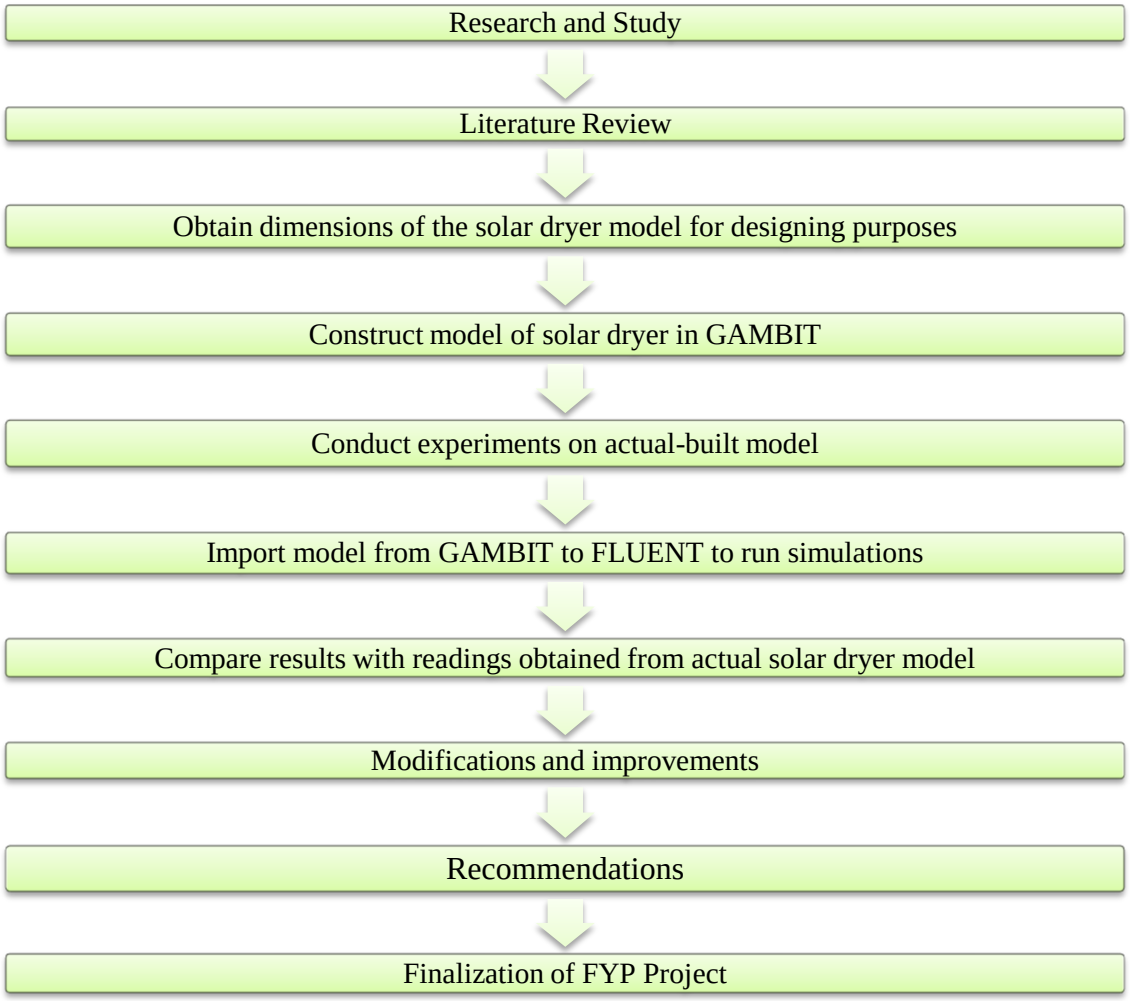

FIGURE 3.2: Flowchart of project flow

3.3 GANTT CHART

ID	Task Name	Start	Finish	Duration
1	Selection of Project Topic	7/21/2008	7/25/2008	.71w
2	Project Title Approval	7/26/2008	7/30/2008	.71w
3	Research on history & types of solar dryers	7/31/2008	8/5/2008	.86w
4	Research on how solar dryers work	8/6/2008	8/14/2008	1.29w
5	Submission of Preliminary Report	8/15/2008	8/15/2008	0w
6	Research on previous works on Solar Hybrid Dryers	8/16/2008	8/19/2008	.57w
7	Gambit session with Graduate Assistant (GA)	8/20/2008	8/20/2008	.14w
8	Literature Review based on previous works	8/21/2008	9/2/2008	1.86w
9	FLUENT session with Graduate Assistant (GA)	9/3/2008	9/3/2008	.14w
10	Research on theoretical equations concerning the drying process	9/4/2008	9/11/2008	1.14w
11	Submission of Progress Report	9/12/2008	9/12/2008	.14w
12	Start on solar dryer modeling using GAMBIT	9/13/2008	9/18/2008	.86w
13	Seminar	9/19/2008	9/19/2008	0w
14	Continue with FLUENT & GAMBIT modeling	9/20/2008	9/26/2008	1w
15	Obtain readings from experiments in lab	9/27/2008	9/30/2008	.57w
16	Compare experimental results with simulation	10/1/2008	10/31/2008	4.43w
17	Submission of Interim Report	10/31/2008	10/31/2008	0w
18	Oral Presentation	11/5/2008	11/5/2008	0w

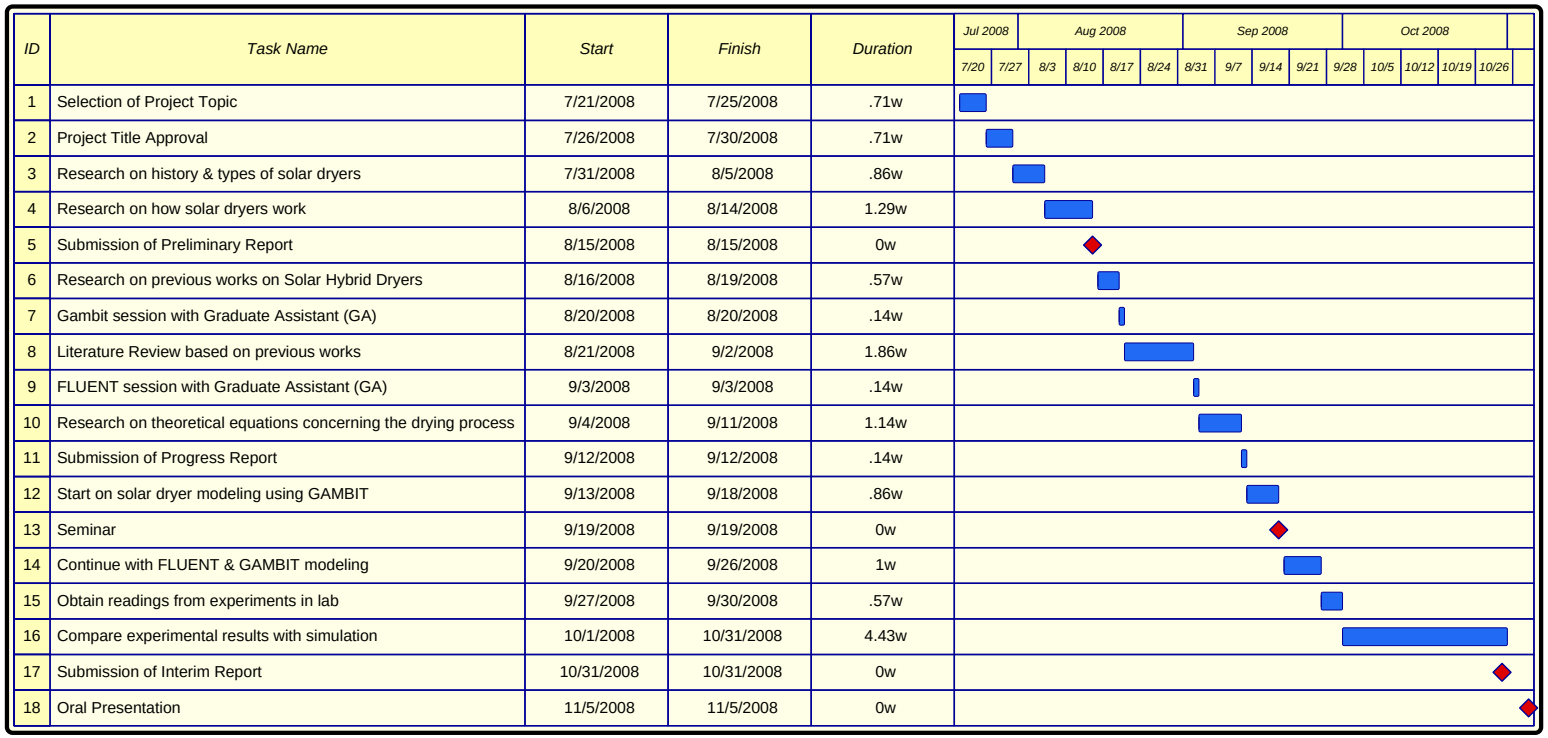

FIGURE 3.3: FYP I Gantt Chart

ID	Task Name	Start	Finish	Duration
1	Work on Navier-Stokes Equations	1/19/2009	1/25/2009	1w
2	Work on FLUENT simulations based on drying by solar	1/26/2009	2/12/2009	2.57w
3	Submission of Progress Report I	2/13/2009	2/13/2009	0w
4	Improve FLUENT simulations based on drying by solar	2/14/2009	2/20/2009	1w
5	Work on FLUENT simulations based on drying by biomass	2/21/2009	3/1/2009	1.29w
6	Research on how to add moisture from surroundings to solar dryer model	3/2/2009	3/12/2009	1.57w
7	Submission of Progress Report II	3/13/2009	3/13/2009	0w
8	Improve on FLUENT simulations based on drying by biomass heater	3/14/2009	3/20/2009	1w
9	Work on adding moisture from surrounding air to solar dryer model	3/21/2009	3/27/2009	1w
10	Obtain experimental readings of solar dryer	3/30/2009	4/3/2009	.71w
11	Compare experimental and simulation data	4/5/2009	4/14/2009	1.43w
12	Improve and work on any problems concerning solar dryer modeling	4/15/2009	4/28/2009	2w
13	Preparation of Final Report	4/28/2009	5/3/2009	.86w
14	Submission of Final Report (Soft Cover)	5/4/2009	5/4/2009	0w
15	Preparation of Oral Presentation & Finalization of FYP II	5/5/2009	6/2/2009	4.14w
16	Oral Presentation	6/3/2009	6/3/2009	0w
17	Submission of Final Report (Hard Cover)	6/19/2009	6/19/2009	0w

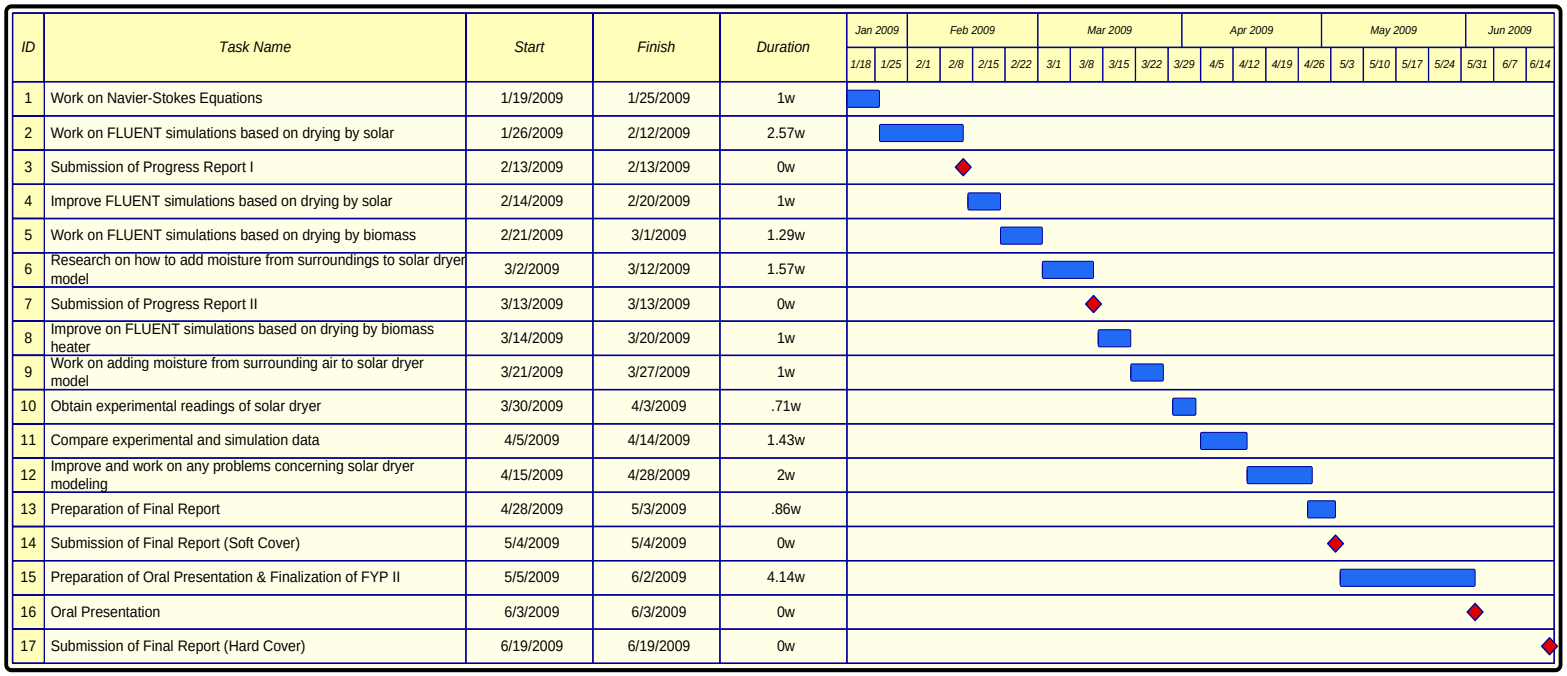

LEGEND

Task bar

Milestone

FIGURE 3.4: FYP II Gantt Chart

3.4 TOOLS

This project is divided into two parts which is numerical and experimental analysis. For numerical analysis, the main software needed are basically just the FLUENT and GAMBIT program. Drawings and documentation are done using AUTOCAD and Microsoft Office.

For the experimental analysis, certain equipments were obtained from the labs. The experiment was conducted with 3 different modes which are by solar radiation, by flue gas from biomass burner and by clean, warm air from biomass burner. Relative humidity and temperature of air was measured using digital hygrometer/psychrometer, temperature of absorber was measured using thermocouple, solar radiation was measured using solarimeter and airflow velocities were measured using anemometer. Refer to Appendix A – Appendix D for figures.

CHAPTER 4
THEORY

This chapter explains the theory of the solar collector and governing equations of the thermo fluid process. The theory of solar collector helps the author obtain a brief understanding on the heat losses and heat gained by the solar collector. The governing equations of the thermo fluid process explain the assumptions made by the author and how these assumptions are applied to the governing equations used in FLUENT.

4.1 THEORY OF SOLAR COLLECTOR

A solar collector is a device for extracting the energy from the sun and converting into a more usable or storable form. During this process, they are heat gained and heat losses occurring on the solar collector.

The energy balance on the absorber is obtained by equating the total heat gained to the total heat loss by the heat absorber of the solar collector [7].

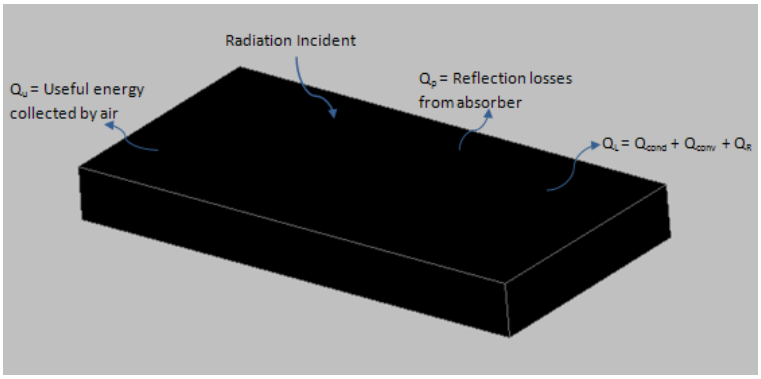

FIGURE 4.1: Energy gain and losses on a solar collector

Therefore,

Total heat gained = Total heat loss

$$IA_c = Q_u + Q_{cond} + Q_{conv} + Q_R + Q_\rho \qquad (1)$$

Where,

I = rate of total radiation incident on the absorber's surface (Wm^{-2});

A_c = collector area (m^2);

Q_u = rate of useful energy collected by the air (W);

Q_{cond} = rate of conduction losses from the absorber (W);

Q_{conv} = rate of convective losses from the absorber (W);

Q_R = rate of long wave re-radiation from the absorber (W);

Q_ρ = rate of reflection losses from the absorber (W).

The three heat loss terms Q_{cond}, Q_{conv} and Q_R are usually combined into one-term (Q_L), i.e.,

$$Q_L = Q_{cond} + Q_{conv} + Q_R \qquad (2)$$

If τ is the transmittance of the top glazing and I_T is the total solar radiation incident on the top surface,

$$IA_c = \tau I_T A_c \qquad (3)$$

The reflected energy from the absorber is given by the expression,

$$Q_\rho = \rho\tau I_T A_c \qquad (4)$$

Where ρ is the reflection coefficient of the absorber

Substitution of Equations (2), (3) and (4) in Eq. (1) yields:

$\tau I_T A_c = Q_u + Q_L + \rho\tau I_T A_c$ Or

$$Q_u = \tau I_T A_c (1 - \rho) - Q_L$$

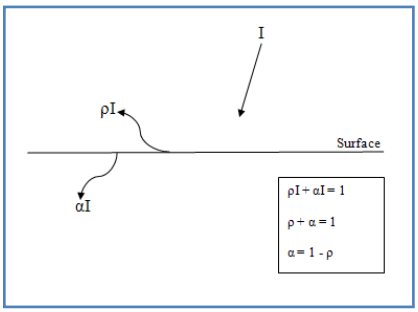

FIGURE 4.2: Radiation entering and escaping surface

From Figure 10, for an absorber, (1 – ρ) = α and hence,

$$Q_u = (\alpha\tau) I_T A_c - Q_L \qquad (5)$$

Where α is solar absorption.

Q_L is composed of conduction, convection and radiation. It is presented in the following form:

$$Q_L = U_L A_c (T_c - T_a) \qquad (6)$$

Where,

U_L = overall heat transfer coefficient of the absorber ($Wm^{-2}K^{-1}$);

T_c = temperature of the collector's absorber (K);

T_a = ambient air temperature (K).

From Equations (5) and (6) the useful energy gained by the collector is expressed as:

$$Q_u = (\alpha\tau) I_T A_c - U_L A_c (T_c - T_{a)} \qquad (7)$$

If the heated air leaving the collector is at collector temperature, the heat gained by the air Q_g is:

$$Q_g = \dot{m}_a C_{pa} (T_c - T_a) \qquad (8)$$

Where,

$\dot{m}$ = mass of air leaving the dryer per unit time (kgs^{-1});

C_{pa} = specific heat capacity of air ($kJkg^{-1}K^{-1}$).

The collector heat removal factor, F_R, is the quantity that relates the actual useful energy gained of a collector, Equation (7), to the useful gained by the air, Equation (9). Therefore,

$$F_R = \frac{Q_g}{Q_u} \qquad (9)$$

$$F_R = \frac{\dot{m}_a C_{pa}(T_c - T_a)}{A_c[\alpha\tau I_T - U_L(T_c - T_a)]} \qquad (10)$$

Or

$$Q_g = A_c F_R[(\alpha\tau)I_T - U_L A_c(T_c - T_a)] \qquad (11)$$

The thermal efficiency of the collector is defined as:

$$n_c = \frac{Q_g}{A_c I_T} \qquad (12)$$

4.2 GOVERNING EQUATIONS OF THE THERMO FLUID PROCESS

4.2.1 Assumptions

Several assumptions are made in modeling the solar dryer model:-

- 2D
- Flow in x and y-direction; u ≠ 0, v≠0
- Steady; $\frac{\partial}{\partial t}$=0
- Compressible; $\boldsymbol{\rho}$ not constant
- Gravity in y-direction; $g_x = 0$

4.2.2 Continuity Equation

$$\cancel{\frac{\partial \rho}{\partial t}} + \frac{\partial(\rho u)}{\partial x} + \frac{\partial(\rho v)}{\partial y} = 0$$

$$\frac{\partial(\rho u)}{\partial x} + \frac{\partial(\rho v)}{\partial y} = 0$$

$$\rho\left(\frac{\partial u}{\partial x} + \frac{\partial v}{\partial y}\right) = 0$$

4.2.3 Conservation of Momentum Equations

(i) x-component

$$\rho\left(\cancel{\frac{\partial u}{\partial t}} + u\frac{\partial u}{\partial x} + v\frac{\partial u}{\partial y}\right) = \cancel{\rho g_x} - \frac{\partial p}{\partial x} + \mu\left(\frac{\partial^2 u}{\partial x^2} + \frac{\partial^2 u}{\partial y^2}\right)$$

$$\rho\left(u\frac{\partial u}{\partial x} + v\frac{\partial u}{\partial y}\right) = -\frac{\partial p}{\partial x} + \mu\left(\frac{\partial^2 u}{\partial x^2} + \frac{\partial^2 u}{\partial y^2}\right)$$

(ii) y-component

$$\rho\left(\cancel{\frac{\partial v}{\partial t}} + u\frac{\partial v}{\partial x} + v\frac{\partial v}{\partial y}\right) = \rho g_y - \frac{\partial p}{\partial y} + \mu\left(\frac{\partial^2 v}{\partial x^2} + \frac{\partial^2 v}{\partial y^2}\right)$$

$$\rho\left(u\frac{\partial v}{\partial x} + v\frac{\partial v}{\partial y}\right) = \rho g_y - \frac{\partial p}{\partial y} + \mu\left(\frac{\partial^2 v}{\partial x^2} + \frac{\partial^2 v}{\partial y^2}\right)$$

4.2.4 Conservation of Energy Equation

$$\frac{\partial}{\partial t}\left[\rho\left(e+\frac{1}{2}v^2\right)\right]+\frac{\partial}{\partial x}\left[\rho u\left(e+\frac{1}{2}v^2\right)\right]+\frac{\partial}{\partial y}\left[\rho v\left(e+\frac{1}{2}v^2\right)\right]=-\frac{\partial \mathrm{q_x}}{\partial \mathrm{x}}-\frac{\partial \mathrm{q_y}}{\partial \mathrm{y}}+$$
$$\frac{\partial}{\partial x}\left(u\sigma_{xx}+v\sigma_{\mathrm{xy}}\right)+\frac{\partial}{\partial y}\left(u\sigma_{yx}+v\sigma_{\mathrm{yy}}\right)+\rho u g_x+\rho u g_y$$

$$\frac{\partial}{\partial x}\left[\rho u\left(e+\frac{1}{2}v^2\right)\right]+\frac{\partial}{\partial y}\left[\rho v\left(e+\frac{1}{2}v^2\right)\right]=-\frac{\partial \mathrm{q_x}}{\partial \mathrm{x}}-\frac{\partial \mathrm{q_y}}{\partial \mathrm{y}}+\frac{\partial}{\partial x}\left(u\sigma_{xx}+v\sigma_{\mathrm{xy}}\right)+$$
$$\frac{\partial}{\partial y}\left(u\sigma_{yx}+v\sigma_{\mathrm{yy}}\right)+\rho u g_y$$

4.2.5 State Equation

$\rho V = mRT$ Or

$$\rho = \frac{P}{RT}$$

CHAPTER 5
NUMERICAL SIMULATION

The numerical analysis is done based on 2 modes of drying which are:-

Scenario 1: Drying by solar energy

Scenario 2: Drying by biomass energy

FIGURES 5.1 and 5.2 shows the labeled GAMBIT solar dryer model based on Scenario 1 and Scenario 2 respectively.

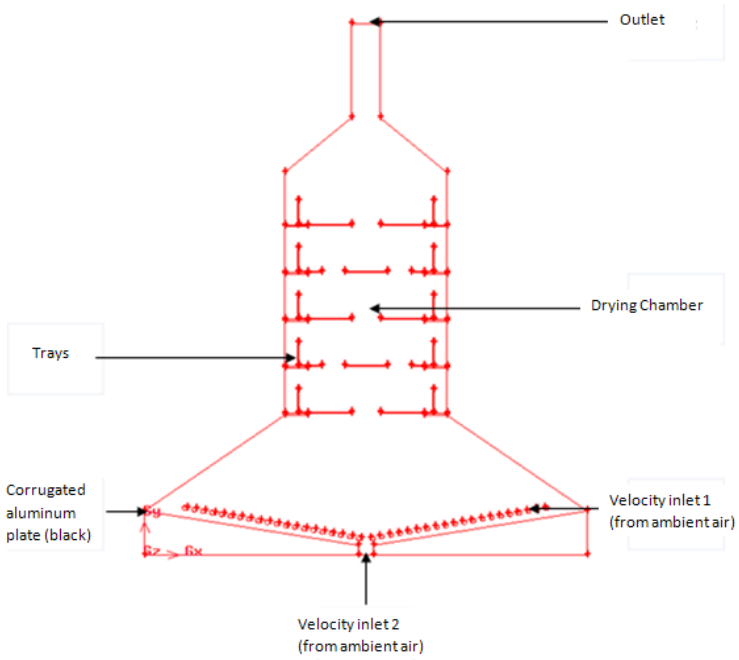

FIGURE 5.1: Labeled GAMBIT solar dryer model based on Scenario 1

For Scenario 1, which is drying by solar energy, the fluid flow is initiated by setting the values for velocity inlets 1 and 2 and also setting the absorber temperature according to experimental values. Temperature distribution at other areas of the dryer and velocity outlet at chimney is observed from simulation results.

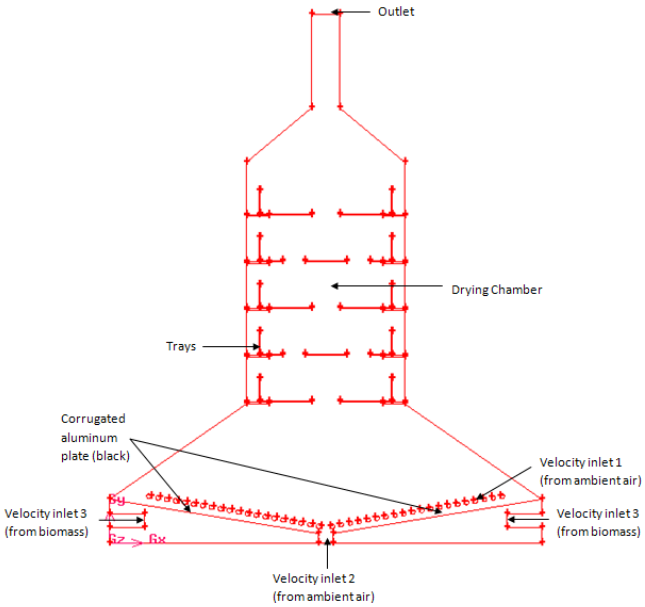

FIGURE 5.2: Labeled GAMBIT solar dryer model based on Scenario 2

For Scenario 2, which is drying by biomass energy, the fluid flow is initiated by setting the values for velocity inlets 1, 2 and 3. Velocity inlet 1 and 2 are both from ambient air, meanwhile, velocity inlet 3 is heated air from the biomass burner. Besides that, temperature at velocity inlet 3 is varied to observe the temperature distribution at other areas of the dryer.

5.1 MODELING CRITERIA

5.1.1 Settings in FLUENT

The solar dryer is modeled based on several settings described below:-

MODELING CRITERIA	SETTINGS
Solver Version	2ddp
Flow Solver	Segregated solver
Viscous model	Standard k-ε model
Solution Controls	SIMPLE, second order upwind discretization

The Solver Version is to specify the dimensionality of the problem. The 2ddp version runs the two-dimensional, double precision solver. The 2ddp version is chosen because it is more accurate compared to the 2d version.

The Flow Solver used is segregated solver. The segregated solver is better for low speed flows while the coupled solver is better for solving transonic or supersonic cases. The segregated solver method also requires less memory than the coupled solver.

The viscous model used is the standard k-ε model. The standard k-ε model is a semi-empirical model based on model transport equations for the turbulent kinetic energy (*k*) and its dissipation rate (ε).

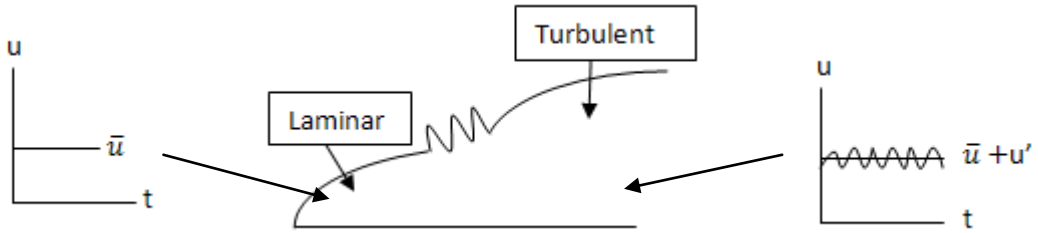

FIGURE 5.3: Laminar to Turbulent Transition.

Flow flows from laminar to turbulent. At turbulent, particles hit each other and lose momentum. This causes fluctuations in velocity at the turbulent part (FIGURE 5.3). Due to fluctuations in velocity, Navier-stokes equations are in the form of $\bar{u} + u'$ and $\bar{v} + v'$. The k-ε model is used to compensate for the fluctuating parts which are u' and v'. Thus, kinematic viscosity, τ is:-

$$\tau = (\mu + \mu_t)\frac{du}{dy}$$

Where $\boldsymbol{\mu}$ is fluid property obtained from table and

$\boldsymbol{\mu}_t$ is turbulent viscosity.

$\boldsymbol{\mu}_t$ is variable to change in shape, Reynolds number, Prandtl number, etc. The “eddy" or turbulent viscosity, $\boldsymbol{\mu}_t$ is computed by combining k and ε as follows:

$$\mu_t = \rho C_\mu \frac{k^2}{\varepsilon}$$

For Solutions Control, FLUENT provides three methods for pressure-velocity coupling in the segregated solver: SIMPLE, SIMPLEC, and PISO. Steady-state calculations will generally use SIMPLE or SIMPLEC, while PISO is recommended for transient calculations. SIMPLE method, which is the default, is used in this case. When the flow is aligned with the grid the first-order upwind discretization may be acceptable. When the flow is not aligned with the grid, first-order convective discretization increases the numerical discretization error. For triangular and tetrahedral grids, since the flow is never aligned with the grid, you will generally obtain more accurate results by using the second-order discretization. Therefore in this matter, second order upwind is used for better accuracy because model has triangular mesh.

5.1.2 Calculations

To obtain velocity inlet of the model, several calculations has to be made by referring to the velocity outlet attained from experimentation results. This is based on the energy conservation equation where $Q_{in} = Q_{out}$. Based on velocity outlet obtained through experimentation, velocity inlet can be calculated as following:

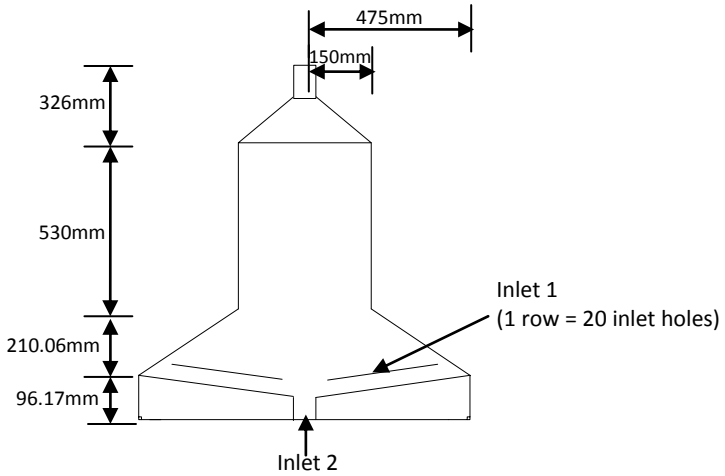

FIGURE 5.4: Graphic Representation of Solar Dryer

2D model in FIGURE 5.4 shows front view of solar dryer. Symmetry on both front and back of solar dryer indicates that they are 4 rows of inlet holes in total. In FIGURE 5.4, 1 row of holes in 2D model represents 2 rows of inlet holes. To obtain velocity flow in each hole:-

$$Q_{in} = Q_{out}$$

$$A_{out} V_{out} = A_{in} V_{in}$$

$$A_{out} V_{out} = A_{in1} V_{in1} + A_{in2} V_{in2}$$

$$A_{out} = \pi(0.03m)^2 = 2.827E-3m^2$$
$$V_{out} = 0.22m/s$$

$$A_{1\ inlet\ \ hole} = \pi(5E-3m)^2 = 7.854E-5m^2$$
$$A_{20\ inlet\ \ holes} = 7.854E-5m^2 x 20 = 1.57E-3m^2$$
$$A_{in1} = 1.57E-3m^2$$

$$A_{in2} = (0.034m\ x\ 1m)^2 = 0.034m^2$$

Substituting,

$$A_{out} V_{out} = 4(A_{in1} V_{in1}) + A_{in2} V_{in2}$$

$$(2.827E-3)(0.22) = 4(1.57E-3)(V_{in1}) + 0.034(V_{in2})$$

$$V_{in1}(for\ 1\ row\ of\ holes) = \frac{(6.2194E-4) - 0.034V_{in2}}{4(1.57E-3)}$$

If V_{in2} is assumed to be 0.0008m/s;

$$V_{in1}(for\ 1\ row\ of\ holes) = \frac{(6.2194E-4) - 0.034(0.0008)}{4(1.57E-3)} = 0.0947\ m/s$$

Therefore,

$$V_{in1}(per\ hole) = \frac{0.0947 * 2}{20} = 0.00947\ m/s$$

$V_{in1}(per\ hole)$ calculated and V_{in2} assumed, is used as velocity inlet boundary conditions in FLUENT.

5.2 MESHING CRITERIA

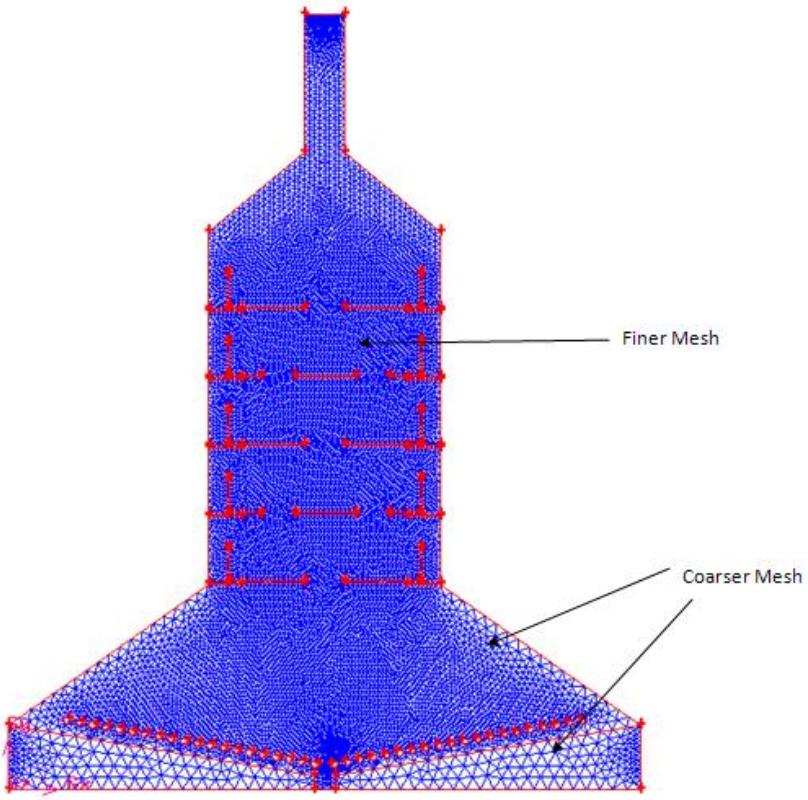

FIGURE 5.5: Mesh on Solar Dryer model

The meshing element used in the model is tri element where mesh includes only triangular mesh elements. The face meshing type is pave meshing meaning an

unstructured grid of mesh elements is created. When a tri-pave meshing scheme is selected, GAMBIT creates a face mesh consisting of irregular triangular elements such as seen in FIGURE 5.5. Notice in FIGURE 5.5 the top part of the solar dryer has a finer mesh compared to the bottom part. Finer mesh is selected at the top because it is the drying chamber and thus, more accurate results are needed. The bottom part is meshed with coarser elements to reduce simulation time.

5.3 BOUNDARY CONDITIONS

5.3.1 Boundary Conditions for simulation of solar dryer based on Scenario 1

The following table shows the boundary conditions for simulating solar dryer based on Scenario 1: Drying with solar energy. A more thorough list of boundary conditions is stated in Appendix E (material properties) and Appendix F (boundary conditions):-

TABLE 5.1: Boundary Conditions for Scenario 1

Zone	Boundary Conditions	Specifications
Velocity Inlet 1	Velocity Inlet	- Velocity Magnitude: 0.009471 m/s - Temperature: 301.7 K
Velocity Inlet 2	Velocity Inlet	- Velocity Magnitude: 0.0008 m/s - Temperature: 301.7 K
Outlet	Pressure Outlet	- Gauge Pressure: 0 - Backflow Total Temperature: 301.7K
Aluminum absorber	Radiator	- Loss coefficient: 3 - Heat Transfer Coefficient: 25 $W/m^2.K$ - Temperature: 343 K
Trays	Wall	- Thermal conditions: Coupled - Wall Thickness: 3mm - Heat Generation Rate: $0W/m^3$
Perspex cover	Wall	- Heat Transfer Coefficient: 6 $W/m^2.K$ - Free Stream Temperature: 301.7 K - Thickness: 3mm

Plastic chimney	Wall	- Heat Transfer Coefficient: 1.1 $W/m^2.K$ - Free Stream Temperature: 301.7 K - Thickness: 3mm

5.3.2 Boundary Conditions for simulation of solar dryer based on Scenario 2

The following table shows the boundary conditions for simulating solar dryer based on Scenario 2: Drying with biomass energy. A more thorough list of boundary conditions is stated in Appendix G (material properties) and Appendix H (boundary conditions):-

TABLE 5.2: Boundary Conditions for Scenario 2

Zone	Boundary Conditions	Specifications
Velocity Inlet 1	Velocity Inlet	- Velocity Magnitude: 0.006315 m/s - Temperature: 303K
Velocity Inlet 2	Velocity Inlet	- Velocity Magnitude: 0.0008 m/s - Temperature: 303K
Velocity Inlet 3	Velocity Inlet	- Velocity Magnitude: 0.25 m/s - Temperature: 338 K
Outlet	Pressure Outlet	- Gauge Pressure: 0 - Backflow Total Temperature: 303K
Aluminum absorber	Wall	- Thermal Conditions: Coupled - Wall Thickness: 5mm - Heat Generation Rate: 0 W/m^3
Trays	Wall	- Thermal conditions: Coupled - Wall Thickness: 3mm - Heat Generation Rate: 0W/m^3
Perspex cover	Wall	- Heat Transfer Coefficient: 6 $W/m^2.K$ - Free Stream Temperature: 303 K - Thickness: 3mm
Plastic chimney	Wall	- Heat Transfer Coefficient: 1.1 $W/m^2.K$ - Free Stream Temperature: 303 K - Thickness: 3mm

CHAPTER 6
RESULTS

Following sections explain the results obtained by simulations and experimental works. Results focusing on flow patterns and temperature distribution are considered.

6.1 SIMULATION RESULTS

6.1.1 Simulation Results based on Scenario 1

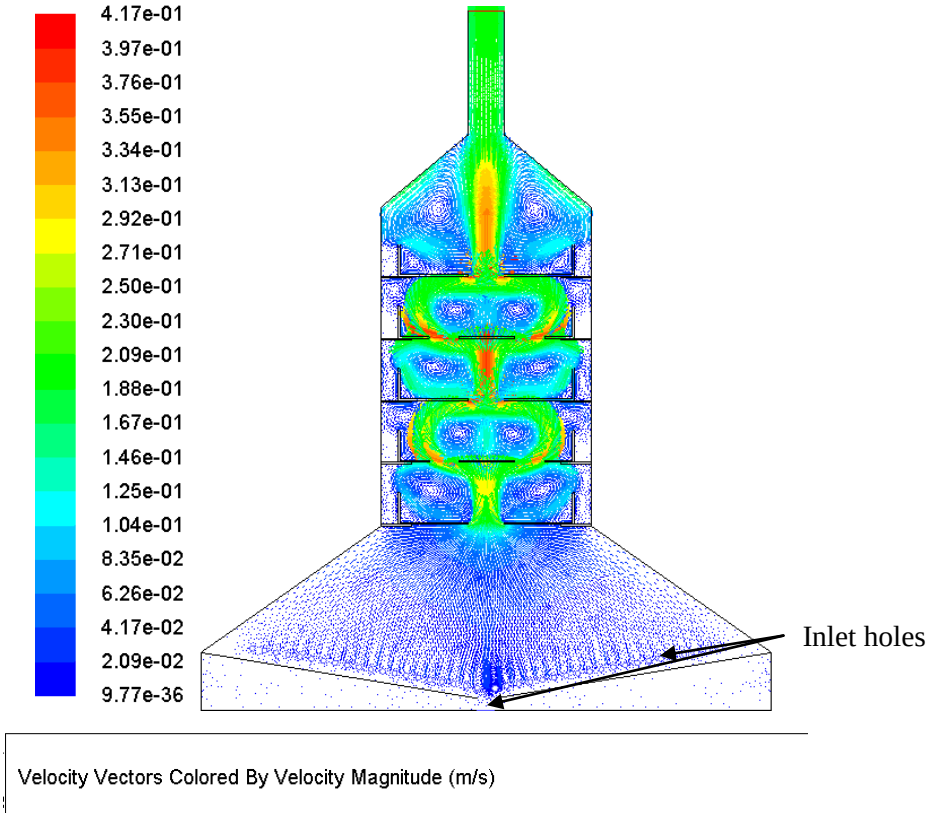

FIGURE 6.1: Velocity Vector of fluid flow based on Scenario 1

FIGURE 6.1 shows the velocity of air flow in the solar dryer. Air flows from ambient air through hole-openings at the base of the solar dryer and out the chimney. From simulation results, velocity of air escaping chimney is shown to be 0.20479 m/s. This is approximately the same as the velocity obtained through experiments in the lab which is 0.22 m/s.

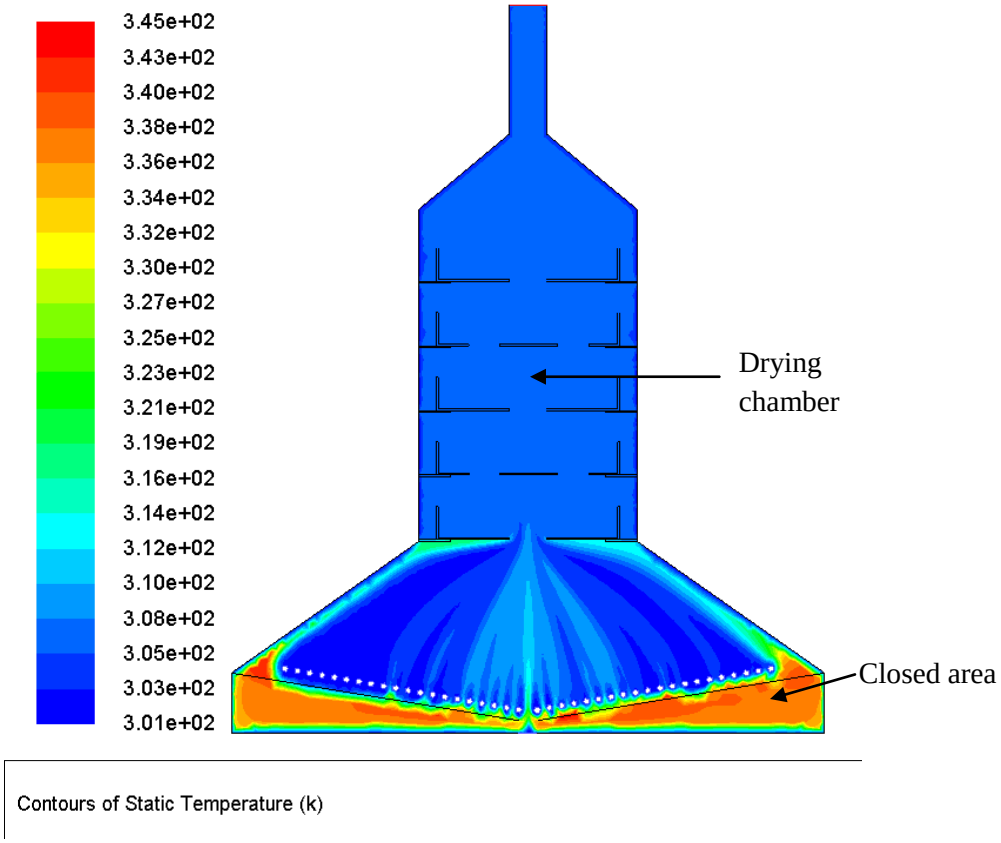

FIGURE 6.2: Temperature Contours based Scenario 1

FIGURE 6.2 shows the temperature distribution in the solar dryer. It can be seen that temperature is highest at areas close to the aluminum absorber. This is due to static velocity in the closed area causing no air circulation and thus high temperature. In the drying chamber, the temperature is 307.65K. As we can in FIGURE 6.2, the temperature distribution is restricted due to the small openings of the trays. In FIGURE 6.1, which shows the velocity vectors, we can observe that the velocity is very high at the small openings and does not distribute evenly at the drying chambers. Due to that, the temperature cannot be distributed upwards and is concentrated only at the bottom.

Therefore, author would recommend the tray openings to be larger in order to increase temperature in the drying chamber.

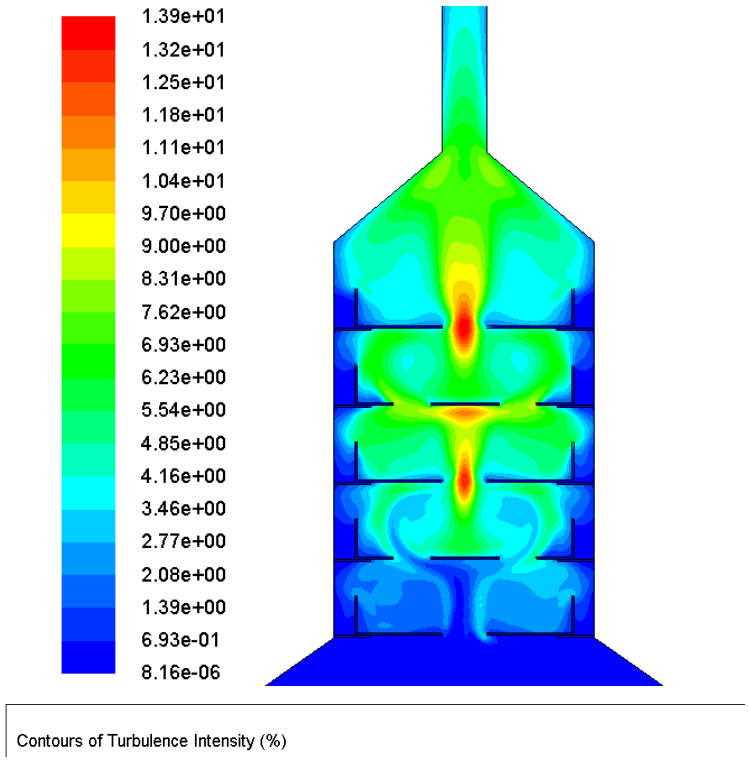

FIGURE 6.3: Turbulence Intensity Contours based on Scenario 1

Turbulence Intensity is defined as the ratio of root mean square of velocity fluctuations, u' to mean flow velocity, u_{avg}.

$$I = \frac{u'}{u_{avg}}$$

Turbulence intensity of 1% or less is generally considered low and turbulence intensity greater than 10% are considered high. FIGURE 6.3 shows high turbulence intensity at the drying chamber as air passes through tray openings. Due to very high turbulence, temperature cannot be distributed properly, as mentioned in the above paragraph. Therefore, author would recommend the tray openings to be larger in order to increase temperature in the drying chamber.

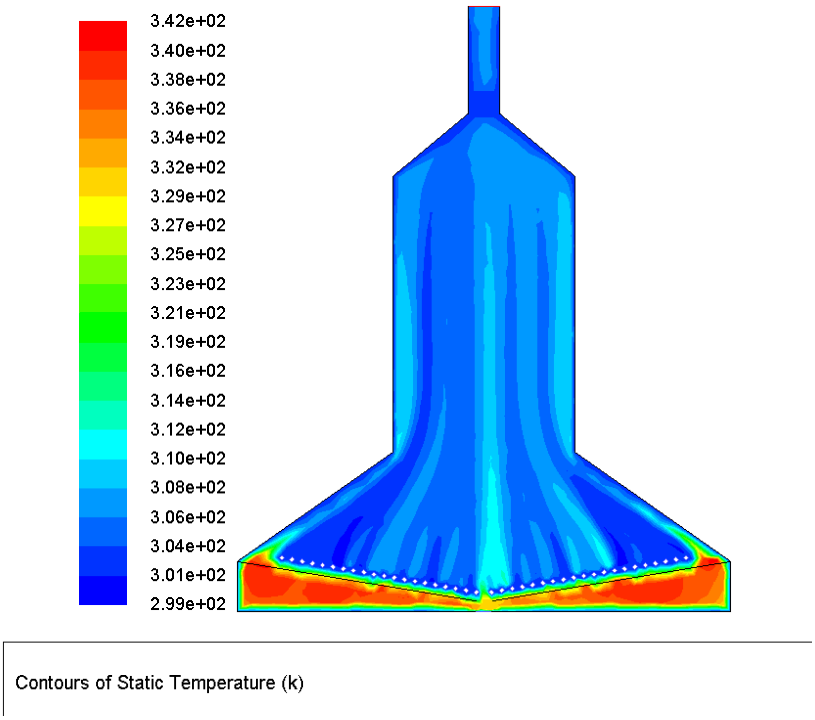

FIGURE 6.4: Solar dryer design without trays

As shown in FIGURE 6.4 above, simulation results shows that when the tray openings are enlarged, there is a more even distribution of temperature in the drying chamber.

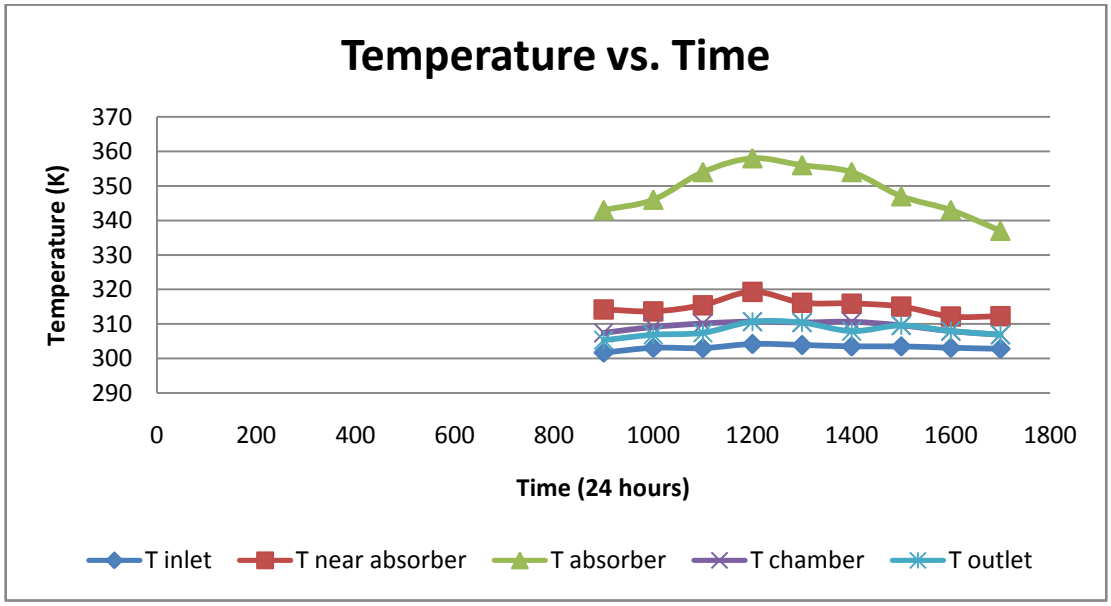

FIGURE 6.5: Summary of temperatures in different areas of the solar dryer based on Scenario 1

FIGURE 6.5 summarizes the simulation results at different locations of the solar dryer. Refer Appendix I for table of simulation data. The simulation is done by initializing the velocity inlets and setting the absorber temperature. The velocity inlet is calculated from the velocity outlet measured during the experiment. Calculation is shown in Chapter 5 of this report. Temperature of absorber is obtained from experiments.

From the results in FIGURE 6.5, we can observe that at high absorber temperature, temperatures in other parts of the solar dryer increases and decreases correspondingly and the trend is similar. However, even though the absorber temperature is high, the temperature does not show a significant rise in other areas. This may be due to the inlet holes situated above the absorber which restricts temperature distribution. By removing the inlet holes, leaving only 1 inlet opening at the bottom of the dryer, it can be observed that temperature is distributed more evenly (FIGURE 6.6) Temperature at chamber for new design is approximately 335 K compared to 307.65 K of previous design.

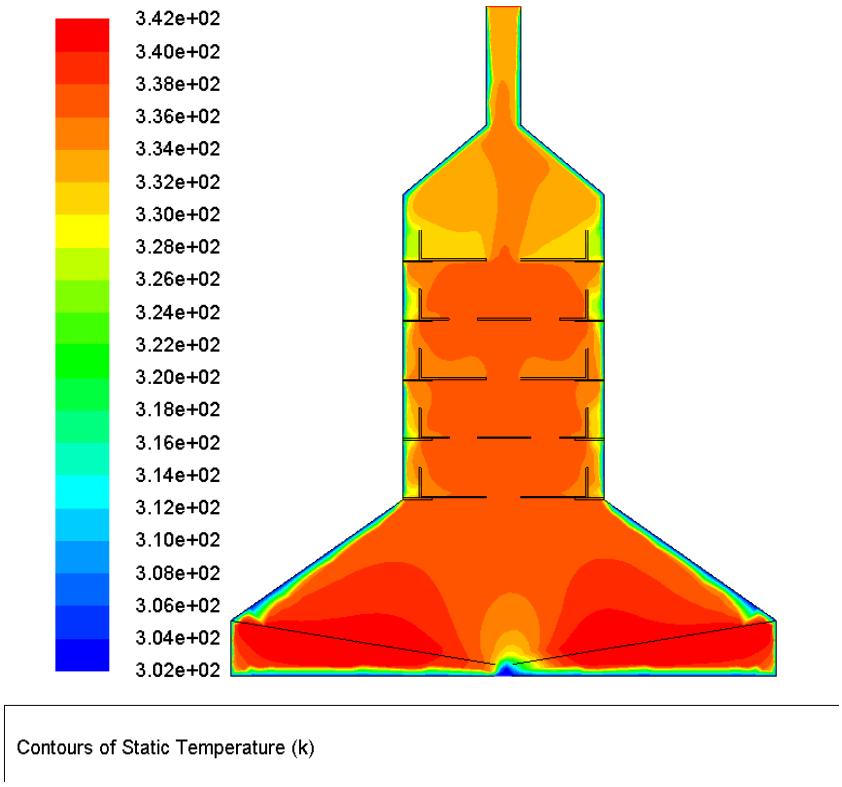

FIGURE 6.6: Solar dryer design without inlet holes and leaving only 1 inlet at bottom of dryer.

6.1.2 Simulation Results based on Scenario 2

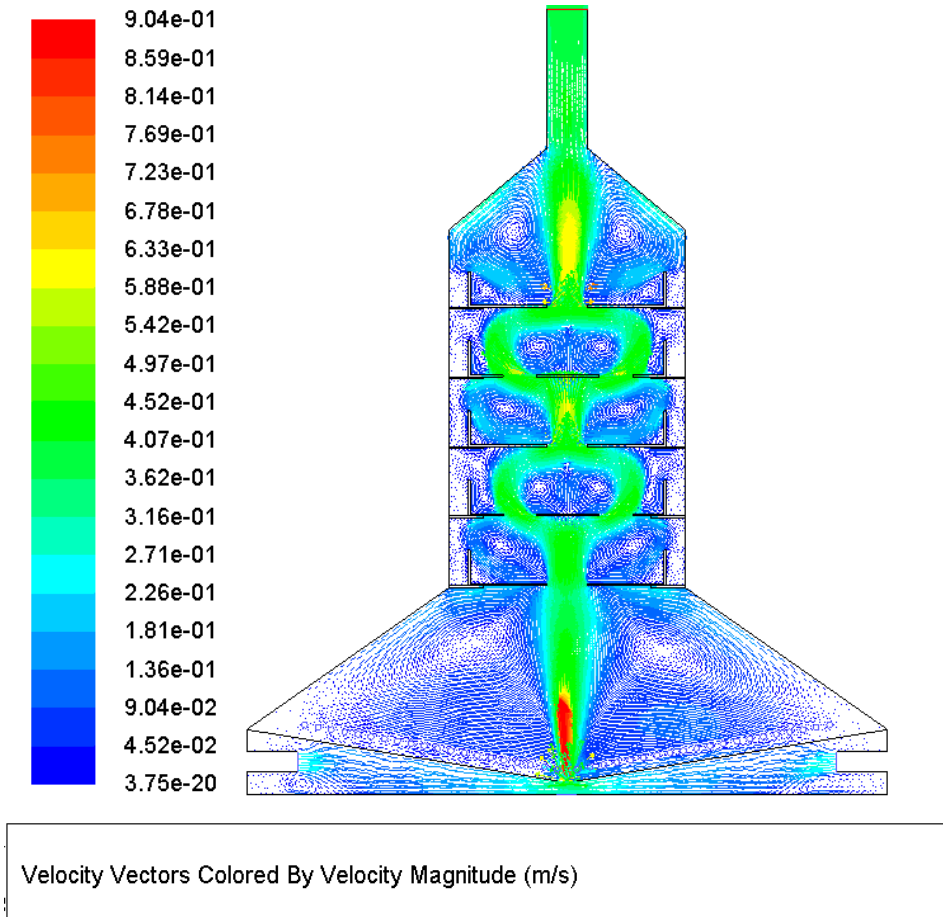

FIGURE 6.7: Velocity Vector of fluid flow based on Scenario 2

FIGURE 6.7 shows the velocity of air flow in the solar dryer. Air flows from the inlet of the biomass burner, through the chamber and out the chimney. From simulation results, it shows that velocity of air escaping chimney is shown to be 0.397 m/s. This is approximately the same as the velocity obtained through experiments in the lab which is 0.4 m/s.

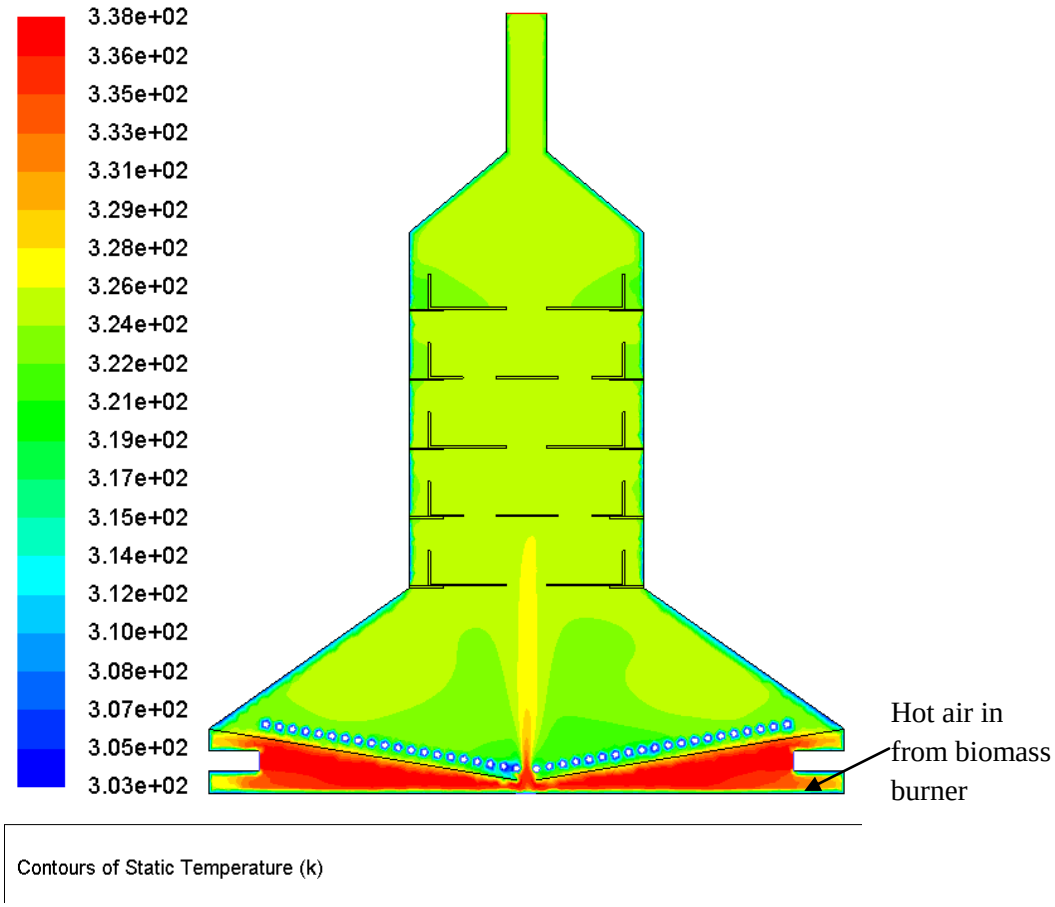

FIGURE 6.8: Temperature Contours based Scenario 2

Figure 6.8 shows the total temperature distribution in the solar dryer. It can be seen that temperature is highest at areas close to the aluminum absorber. This is due to the hot air flow from the biomass burner. In the drying chamber, the temperature is 324.08K. Thus value is close to the experimental value of the drying chamber which is 316.1K. Temperature distribution is more even if compared the simulation based on drying by solar energy because of the stronger air flow in the inlet, thus enabling a smoother distribution of temperature throughout the solar dryer. However, temperature distribution can be improved by enlarging the tray openings as shown in FIGURE 6.4.

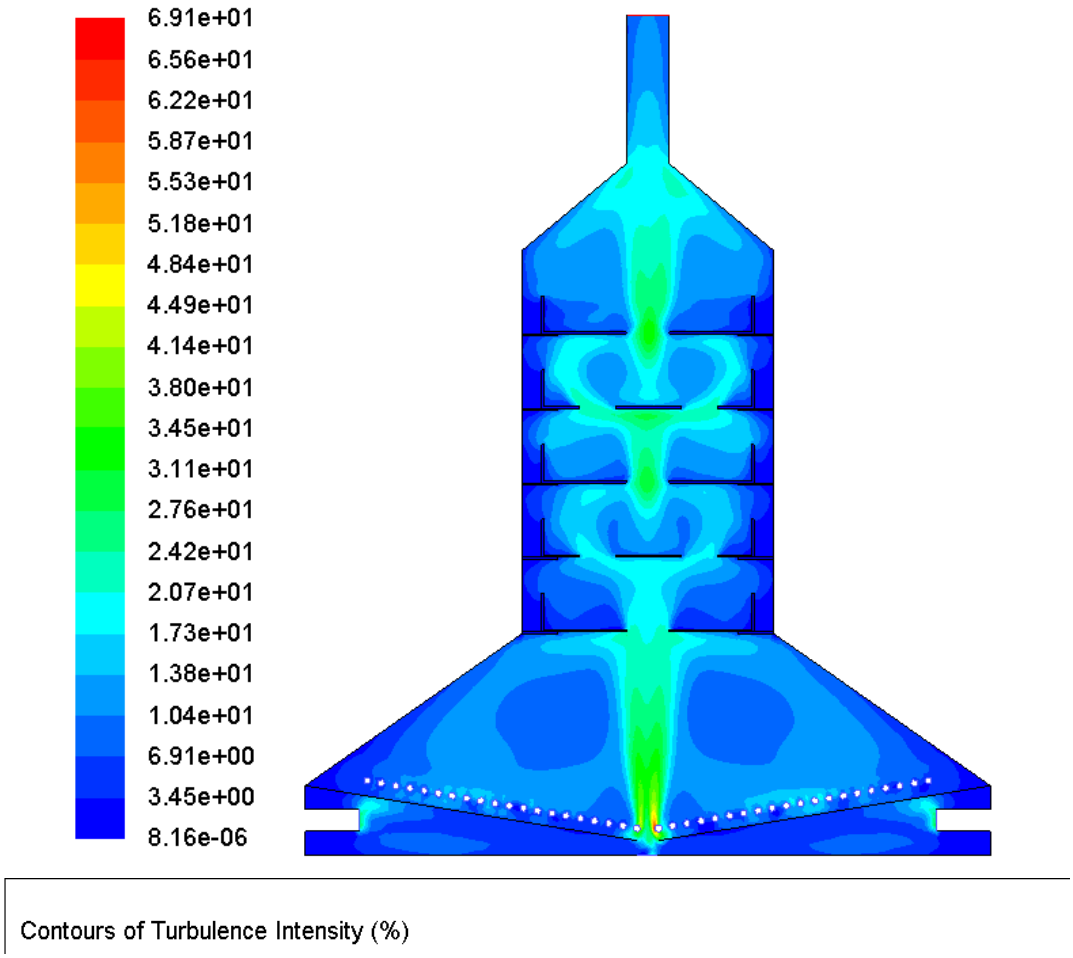

FIGURE 6.9: Turbulence Intensity Contours based on Scenario 2

Figure 6.9 shows high turbulence intensity at the drying chamber. This is due to the small spacing between the trays. Turbulence can be reduced by enlarging the openings between the trays as shown in FIGURE 6.4.

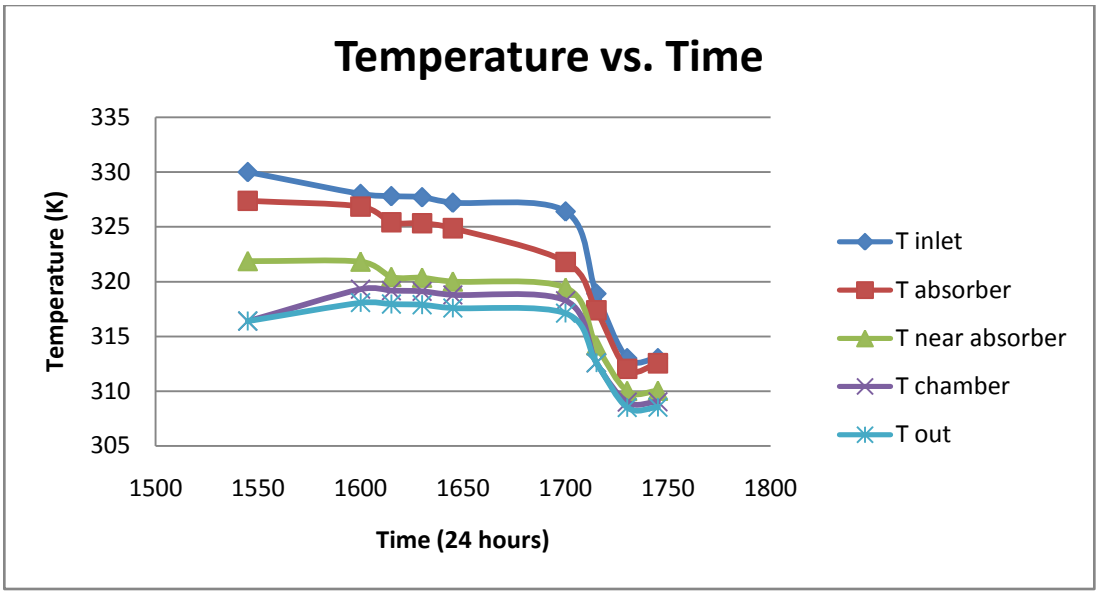

FIGURE 6.10: Summary of temperatures in different areas of the solar dryer based on Scenario 2

FIGURE 6.10 summarizes the simulation results at different locations of the solar dryer. Refer Appendix J for table of simulation data. The simulation is started off by setting the inlet temperature and velocity inlets. The velocity inlet is calculated from the velocity outlet measured during the experiment. Temperature at inlet is obtained from experiments.

From the results in FIGURE 6.10, we can observe that at high inlet temperature, temperatures in other parts of the solar dryer increases and decreases correspondingly and the trend is similar. Temperature at inlet decreases with time causing a decrease in temperature at other areas of the solar dryer simultaneously. Temperature at the inlet can be maintained by observing and controlling the fire in the biomass burner to ensure constant fire and heat.

6.1.3 3D Model

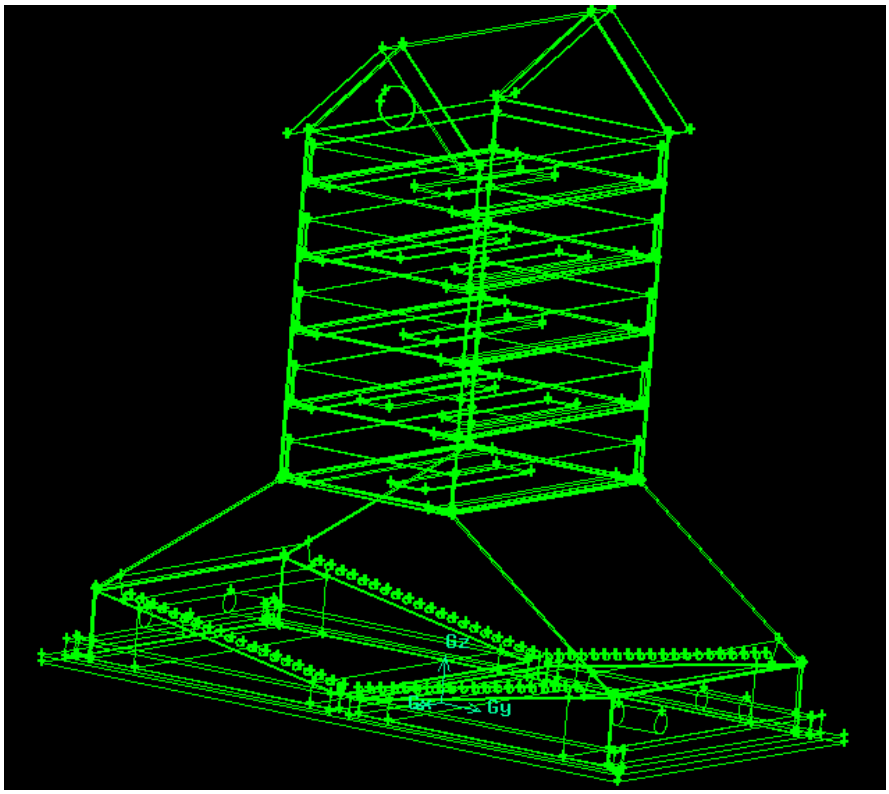

FIGURE 6.11: 3D GAMBIT model of solar dryer

A 3D model of the solar dryer has been constructed using GAMBIT. To further study this project and to obtain more accurate results, this 3D model can be simulated using FLUENT. Results from the 3D model can then be compared with the 2D model and experimental data for a thorough study on this project.

6.1.4 Simulation of dryer with addition of mass flow rate

Simulation of dryer was also conducted with the addition of mass flow rate in the areas shown in Figure 6.12. Parameters used were identical to those used in Scenario 1 except with the addition of mass flow rate. The purpose of incorporating mass flow rate is to represent the moisture of products to be dried. Results from the previous final year student shown in TABLE 6.3 below can be used to calculate specific mass of air.

TABLE 6.3: Data for drying of Empty Fruit Bunch (EFB) [10]

Items	Values
$\dot{m}_{evaporated}$ (kg/s)	$2.208*10^{-5}$
h_{fg} (kJ/kg)	2382.75
C_p (kJ/kg.K)	1.004

$$\dot{m}_{air} = \frac{\dot{m}_{evaporated} * h_{fg}}{C_p(T_{out} - T_{ambient})}$$

From equation above, mass flow rate is known to be 9.529E-3 kg/s. Therefore, due to the 10 inlets shown in Figure 6.12, each inlet has a value of 9.529E-4 kg/s.

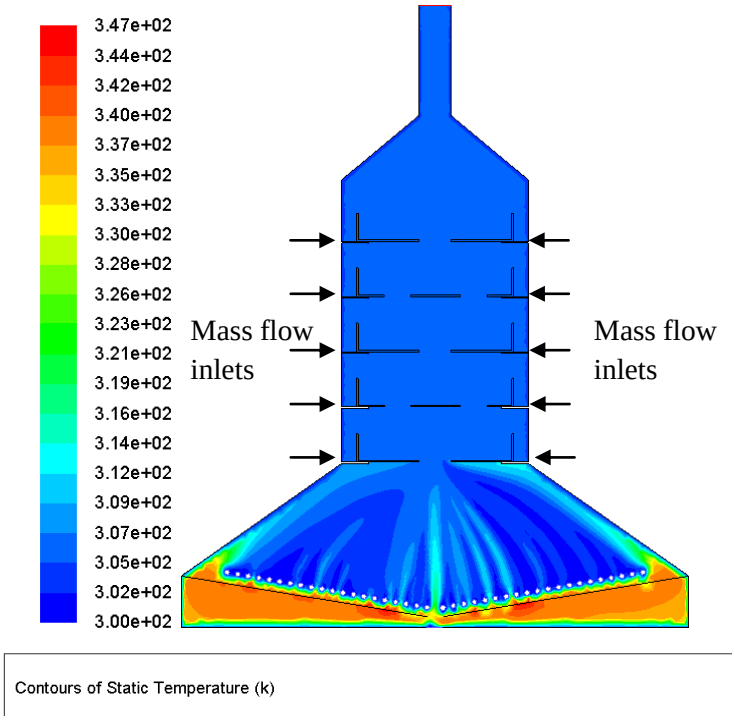

FIGURE 6.12: Temperature Contours of Scenario 1 with additional mass flow rate boundary condition

Based on results obtained from simulation, temperature at chamber is 306.956 K. Temperature is slightly lower compared to simulation without mass flow rate **which is** 307.65K. The temperature is lowered due to the slight addition of the specific mass of air. However, only minimal changes occur because the value of mass flow rate is very low.

6.2 EXPERIMENTAL RESULTS

6.2.1 Experimental Results Based on Scenario 1

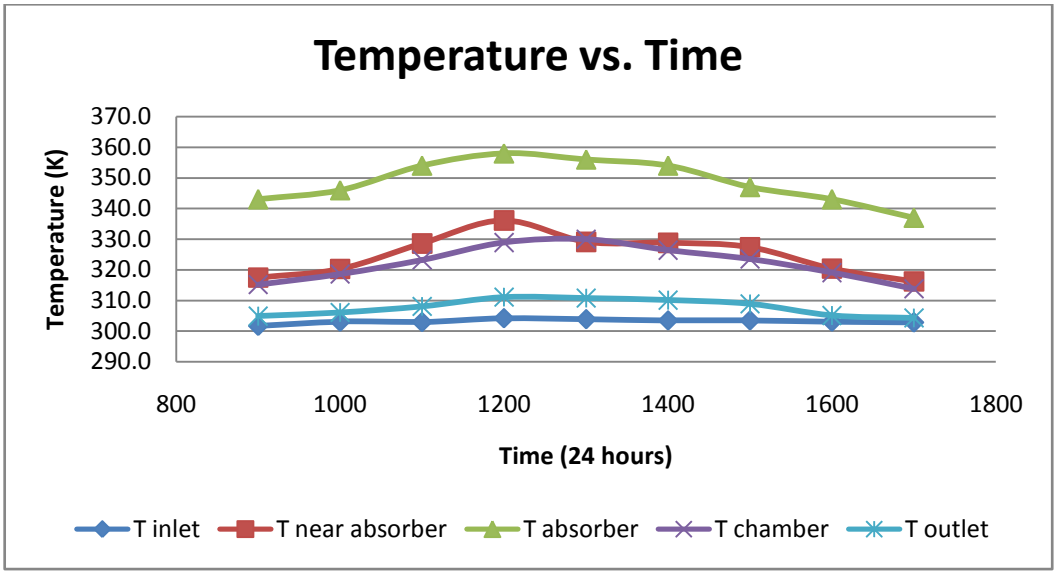

FIGURE 6.13: Summary of Experimental Results of Scenario 1

This experiment was carried out without any products used for drying to test the performance of the solar dryer. It can be observed that as the temperature rises due to the rising solar irradiance, the temperature in all areas of the solar dryer rises simultaneously. From the graph, it is shown that the optimum performance of the dryer is at 1200 hours due to the highest solar irradiation of 725 W/m^2. Refer Appendix K for table of experimental results.

6.2.2 Experimental Results based on Scenario 2

For Scenario 2, which is drying by biomass energy, experimentation is conducted based on two modes which are direct flue from biomass burner and clean, warm air from biomass burner. Direct flue is air directly from coal to dryer and is used from drying waste products, wood chips, etc. Meanwhile, clean, warm air is air which collects heat from coal when passing through a heat exchanger. Clean, warm air is used to dry food products in order to avoid contamination or poison.

6.2.2.1 Direct flue from biomass burner

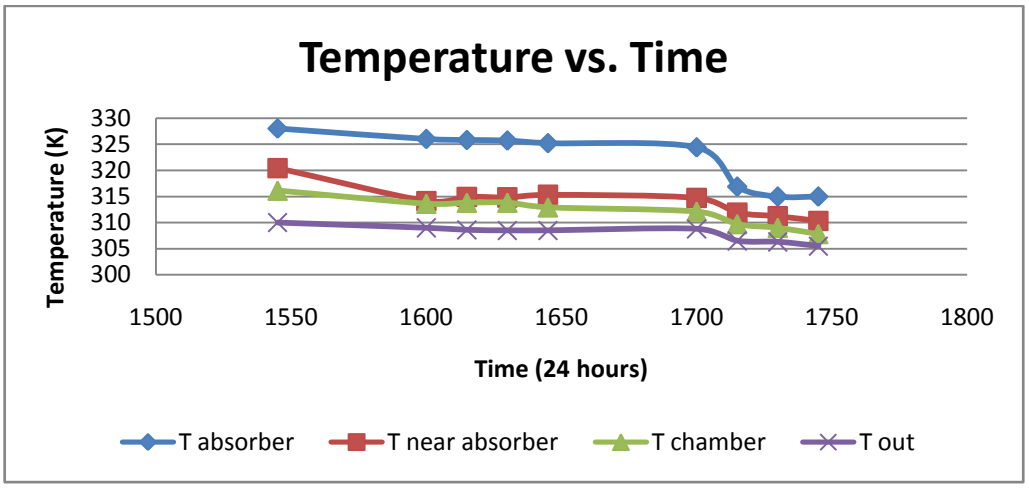

FIGURE 6.14: Summary of Experimental Results of heating by Direct Flue from Biomass Burner

FIGURE 6.13 shows the summary of experimental results by using direct flue from biomass burner as the input. Refer Appendix L for table of experimental results. As the heating process is done from 1550 hours to 1750 hours, there is a constant drop in temperature in the solar dryer. This may be due to inconsistent heat or fire in the biomass burner. Thus, while conducting the experiment, the flame in the biomass burner has to be continuously observed so that the flame will maintain at high heat.

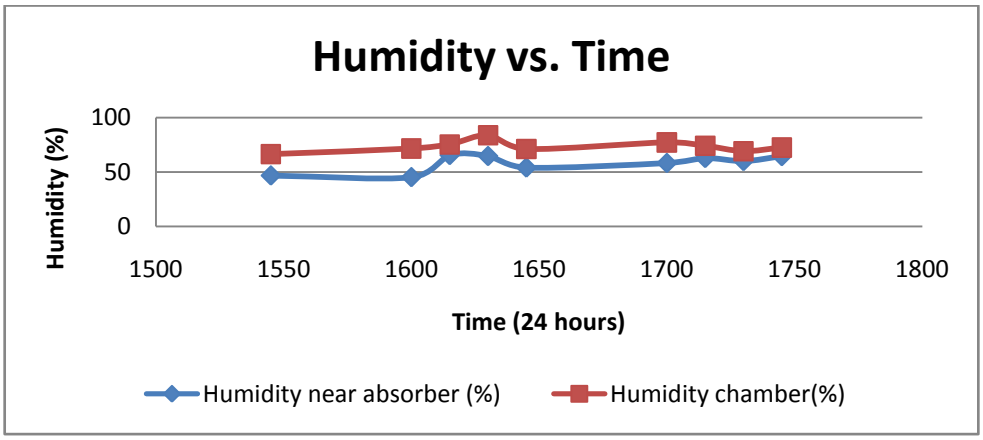

FIGURE 6.15: Comparison of humidity near absorber and humidity at chamber of drying by Direct Flue from Biomass Burner

FIGURE 6.14 shows the comparison of humidity at the area near the absorber and at the drying chamber. It can be observed that the humidity at the drying chamber is higher compared to at the absorber. At the bottom of the drying (absorber area), humidity is low due to high temperature. Dry air then flow upward, removing moisture from food. As higher amount of moisture is absorbed, humidity increases.

6.2.2.2 Clean, warm air through heat exchanger

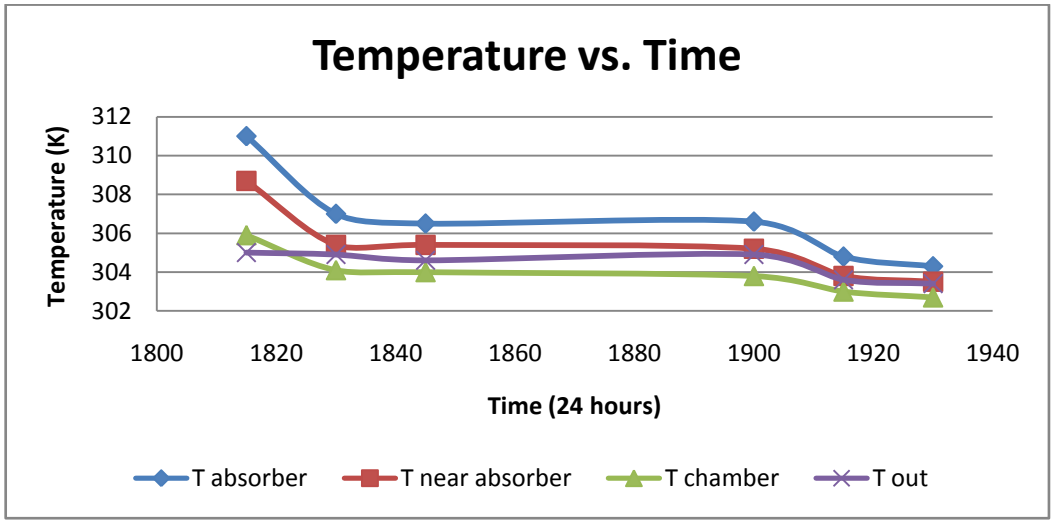

FIGURE 6.16: Summary of Experimental Results of heating by clean, warm air from Biomass Burner

Drying by clean warm air is done by flowing flue gas from biomass burner through a heat exchanger. Hot flue gas then transfers heat to the passing air. In the heat exchanger there is a foil to maintain the heat of the clean air. However from the experimental results observed in Figure 6.15, it shows that the temperature in the solar dryer is very low and not sufficient to heat products. Refer Appendix M for table of experimental results. This may be due to heat losses in the pipes connecting the solar dryer and the biomass burner. It may be also due to improper design of the heat exchanger causing insufficient amount of heat transfer to the passing air.

6.3 COMPARISON BETWEEN SIMULATION AND EXPERIMENTAL RESULTS

The results obtained by experiments and simulations are compared to observe the similarities in both the models. By justifying the fact that both models are similar, further modification can be done to the simulation model to obtain the optimum multipurpose solar dryer without wasting costs by modifying the actual solar dryer model.

6.3.1 Comparison between simulation and experimental results for Scenario 1

The velocity outlet for both simulation and experimental model shows close results with similar trend. Refer Appendix N for graph of velocity comparison. Temperature at chamber for both simulation and experimental model are of the same trend. However, the temperatures for the experimental model are higher if compared to the simulation model. The temperature difference between simulation and experimental data is around 10°C, which is rather large. This may be due to error of experimenting process or error in equipment. Refer Appendix O for graph of temperature comparison.

6.3.2 Comparison between simulation and experimental results for Scenario 2

Velocity at the outlet for both simulation and experimental model shows close results with similar trend when dried by flue gas from biomass. Refer Appendix P for graph of velocity comparison. There is also similar trend and close values for both simulation and experimental data when temperature at chamber is compared. Refer Appendix Q for graph of temperature comparison.

This proves that the design of the model in FLUENT is comparable to the actual built model constructed by the previous FYP student. Therefore, the simulation model can be evaluated and modified in order to obtain the optimum solar dryer design without wasting time and cost by modifying the actual model.

CHAPTER 7
CONCLUSION AND RECOMMENDATIONS

7.1 CONCLUSION

This paper describes simulation of the multipurpose solar dryer using FLUENT and experimentation works to justify the model. Modeling is done based on 2 scenarios – drying by solar energy and drying by biomass energy. Experimentation is done based on 3 modes which are by solar energy, by flue gas from biomass burner and by clean, warm air from biomass burner.

Based on experimentations conducted on drying by solar energy and drying by flue gas, the temperature obtained is not very high but sufficient enough to dry products. However, results show that flue gas from the biomass burner produces more heat compared to drying by solar energy. Therefore, drying by direct flue gas is a more efficient method and results in products of lower moisture content if compared to by solar energy. Nevertheless, this is not applicable for food products because food may be contaminated by poison from flue gases.

Clean, warm air heated by flue gas passing through a heat exchanger is used in the case of drying food products. Nonetheless, the temperature is rather low and insufficient to dry products. This may be due to heat loss in the pipes and connections or due to improper design of heat exchanger.

Besides that, based on simulation results, it can be observed that due to the small openings in the trays, the temperature cannot be distributed thoroughly throughout the drying chamber resulting in low temperatures in the drying chamber.

7.2 RECOMMENDATIONS

The author would like to recommend that the tray openings of the solar dryer be increased to allow sufficient distribution of air flow throughout the drying chamber to enable proper heat distribution. Also, simulation results show that inlet holes at base of the dryer restricts temperature distribution. Therefore, removal of the inlet holes produces higher temperature at other areas of the dryer.

Besides that, to improve the results of drying by clean, warm air, the heat exchanger can be redesigned by increasing the contact area of the heating element in the heat exchanger. The current material used as heat exchanger is a galvanized iron plate. A better material should be used to maximize heat transfer to the passing air. The pipes connecting the burner to the solar dryer can also be shorten and better insulation material be used to reduce heat losses.

The author would also like to recommend for simulation using a 3D model instead of 2D model for more accurate results. Moisture of food and also humidity of air can also be added to the simulation model to obtain a more real-life scenario of the drying process and therewith achieve better results.

REFERENCES

[1] Gordon J., 2001, *Solar Energy - The State of The Art*, London, James & James (Science Publishers) Ltd.

[2] Design and Performance Analysis of solar dryer for banana slices using Scheffler Dish and its comparison with Electrical Food Dryer. Online at http://www.ese.iitb.ac.in/~icaer2007/Latest%20PPT%20File/54_143_TS3%20A.pdf

[3] Drying of Foods. Online at http://www.itdg.org/docs/technical_information_service/drying_of_foods.pdf

[4] Roger G. Gregoire. *Understanding solar food dryers*. VITA report.

[5] The Solar Dryer. Online at http://www.wot.utwente.nl/information/tour/solardryer.html

[6] Trends in solar energy research. Online at http://books.google.com.my/books?id=gpD-M_ZYMVMC&pg=PA173&lpg=PA173&dq=direct+solar+dryer+wavelength&source=web&ots=8Pm2Cd32Gd&sig=VK9c3yESUpY2rZ0VNO2W4nconOg&hl=en&sa=X&oi=book_result&resnum=1&ct=result#PPA173,M1

[7] Bukola O. B., Ayoola, P. O., 2008, "Performance Evaluation of a Mixed-Mode Solar Dryer," *Technical Journal Report* **11(4)**: *225-231*

[8] Serafica, E. and del Mundo, R., "Design and Qualitative of a Hybrid Solar-Biomass Powered Dryer for fish".

[9] Biomass Burners. Online at http://www.alternative-energy.co.uk/Biomass%20Burners.htm

[10] Yusheila Bt Md Yunus 2008, *Hybrid Solar Dryer with Biomass Integration*, Bachelor of Engineering Thesis, University Technology PETRONAS, Malaysia.

[11] Mastekbayeva, G. A., Bhatta C. P., Leon, M. A., Kumar, S., July 1999, "Experimental Studies on a Hybrid Dryer."

[12] Prasad, J., Vijay, V. K., 2005, "Experimental studies on drying of Zingiber officinale, Curcuma longa l. and Tinospora cordifolia in Solar-Biomass Hybrid drier," *Journal of Food Engineering* **75(4)**: *497-502*

[13] Prasad, J., Vijay, V. K., Tiwari, G. N., Sorayan, V. P. S., 2006, "Study on performance evaluation of Hybrid Drier for Turmeric (Curcuma longa L.) drying at village scale," *Journal of Renewable Energy* **75(4)**: 497-502

[14] Gewali, M. B., Joshi, C. B., Bhandari, R., 2005, "Performance Evaluation of a Hybrid Solar Biomass Cabinet Dryer," *European Journal of Scientific Research* **4(1)**: 23-33

[15] Thanaraj, T., Dharmasena D. A. N., Samarajeewa, U., 2004, "Development of a Rotary Solar Hybrid Dryer for Small Scale Copra Processing," *Tropical Agriculture Research* **16**: 30-315

[16] Koonsrisuk, A., Chitsomboom, T., 2007, "Dynamic Similarity in Solar Chimney Modeling," *Solar Energy* **81(12)**: 1439-1446

[17] Therdtai, N., Zhou, W., Adamczak, T., 2004, "Three-dimensional CFD modelling and simulation of the temperature profiles and airflow patterns during a continuous industrial baking process," *Journal of Food Engineering* **65(4)**: 599-608

APPENDICES

APPENDIX A – Digital Hygrometer/ Psychrometer

APPENDIX B – Solarimeter

APPENDIX C – Anemometer

APPENDIX D – Thermocouple

APPENDIX E – Material Properties specifications in FLUENT by drying with solar energy

APPENDIX F – Boundary Conditions specifications in FLUENT by drying with solar energy

APPENDIX G - Material Properties specifications in FLUENT by drying with biomass energy

APPENDIX H - Boundary Conditions specifications in FLUENT by drying with biomass energy

APPENDIX I – Simulation Data for Scenario 1(Solar Energy)

APPENDIX J – Simulation Data for Scenario 2 (Biomass Energy)

APPENDIX K – Experimental Data for Scenario 1 (Solar Energy)

APPENDIX L - Experimental Data for Scenario 2 (Flue Gas)

APPENDIX M - Experimental Data for Scenario 2 (Clean, warm air)

APPENDIX N - Comparison of velocity outlet for simulation and experimental model for Scenario 1 (Solar Energy)

APPENDIX O - Comparison of temperature in chamber for simulation and experimental data for Scenario 1 (Solar Energy)

APPENDIX P - Comparison of velocity outlet for simulation and experimental model for Scenario 2 (Biomass energy)

APPENDIX Q - Comparison of temperature in chamber for simulation and experimental data for Scenario 2 (Biomass energy)

APPENDIX A

Digital Hygrometer/Psychrometer

APPENDIX B

Solarimeter

APPENDIX C

Anemometer

APPENDIX D

Thermocouple

APPENDIX E

Material Properties

Material: pvc (solid)

Property	Units	Method	Value(s)
Density	kg/m3	constant	1410
Cp (Specific Heat)	j/kg-k	constant	900
Thermal Conductivity	w/m-k	constant	0.19

Material: perspex (solid)

Property	Units	Method	Value(s)
Density	kg/m3	constant	1150
Cp (Specific Heat)	j/kg-k	constant	1450
Thermal Conductivity	w/m-k	constant	0.25

Material: air (fluid)

Property	Units	Method	Value(s)
Density	kg/m3	constant	1.225
Cp (Specific Heat)	j/kg-k	constant	1006.43
Thermal Conductivity	w/m-k	constant	0.0242
Viscosity	kg/m-s	constant	1.7894001e-05
Molecular Weight	kg/kgmol	constant	28.966
L-J Characteristic Length	angstrom	constant	3.711
L-J Energy Parameter	k	constant	78.6
Thermal Expansion Coefficient	1/k	constant	0
Degrees of Freedom		constant	0
Speed of Sound	m/s	none	#f

Material: aluminum (solid)

Property	Units	Method	Value(s)
Density	kg/m3	constant	2719
Cp (Specific Heat)	j/kg-k	constant	871
Thermal Conductivity	w/m-k	constant	202.39999

APPENDIX F

```
Boundary Conditions
-------------------

   Zones

      name                id   type
      ---------------------------------------
      fluid               2    fluid
      plates-shadow       12   wall
      wall                3    wall
      velocity_inlet2     4    velocity-inlet
      plates              5    wall
      aluminum            6    radiator
      outlet              7    pressure-outlet
      wall_plastic        8    wall
      velocity_inlet      9    velocity-inlet
      default-interior    11   interior
      plates:001          1    wall

   Boundary Conditions

      fluid

         Condition                                                  Value
         ---------------------------------------------------------------
         Material Name                                              air
         Specify source terms?                                      no
         Source Terms                                               ()
         Specify fixed values?                                      no
         Fixed Values                                               ()
         Motion Type                                                0
         X-Velocity Of Zone                                         0
         Y-Velocity Of Zone                                         0
         Rotation speed                                             0
         X-Origin of Rotation-Axis                                  0
         Y-Origin of Rotation-Axis                                  0
         Deactivated Thread                                         no
         Laminar zone?                                              no
         Set Turbulent Viscosity to zero within laminar zone?       no
         Porous zone?                                               no
         X-Component of Direction-1 Vector                          1
```

Y-Component of Direction-1 Vector	0
Direction-1 Viscous Resistance	0
Direction-2 Viscous Resistance	0
Direction-1 Inertial Resistance	0
Direction-2 Inertial Resistance	0
C0 Coefficient for Power-Law	0
C1 Coefficient for Power-Law	0
Porosity	1
Solid Material Name	aluminum

plates-shadow

Condition	Value
Wall Thickness	0.003
Heat Generation Rate	0
Material Name	perspex
Thermal BC Type	3
Temperature	300
Heat Flux	0
Convective Heat Transfer Coefficient	0
Free Stream Temperature	300
Wall Motion	0
Shear Boundary Condition	0
Define wall motion relative to adjacent cell zone?	yes
Apply a rotational velocity to this wall?	no
Velocity Magnitude	0
X-Component of Wall Translation	1
Y-Component of Wall Translation	0
Define wall velocity components?	no
X-Component of Wall Translation	0
Y-Component of Wall Translation	0
External Emissivity	1
External Radiation Temperature	300
Wall Roughness Height	0
Wall Roughness Constant	0.5
Rotation Speed	0
X-Position of Rotation-Axis Origin	0
Y-Position of Rotation-Axis Origin	0
X-component of shear stress	0
Y-component of shear stress	0

Surface tension gradient	0
Specularity Coefficient	0

wall

Condition	Value
Wall Thickness	0.003
Heat Generation Rate	0
Material Name	perspex
Thermal BC Type	2
Temperature	300
Heat Flux	0
Convective Heat Transfer Coefficient	6
Free Stream Temperature	301.70001
Wall Motion	0
Shear Boundary Condition	0
Define wall motion relative to adjacent cell zone?	yes
Apply a rotational velocity to this wall?	no
Velocity Magnitude	0
X-Component of Wall Translation	1
Y-Component of Wall Translation	0
Define wall velocity components?	no
X-Component of Wall Translation	0
Y-Component of Wall Translation	0
External Emissivity	1
External Radiation Temperature	300
Wall Roughness Height	0
Wall Roughness Constant	0.5
Rotation Speed	0
X-Position of Rotation-Axis Origin	0
Y-Position of Rotation-Axis Origin	0
X-component of shear stress	0
Y-component of shear stress	0
Surface tension gradient	0
Specularity Coefficient	0

velocity_inlet2

Condition	Value
Velocity Specification Method	2

Reference Frame	0
Velocity Magnitude	0.00079999998
X-Velocity	0
Y-Velocity	0
X-Component of Flow Direction	1
Y-Component of Flow Direction	0
X-Component of Axis Direction	1
Y-Component of Axis Direction	0
Z-Component of Axis Direction	0
X-Coordinate of Axis Origin	0
Y-Coordinate of Axis Origin	0
Z-Coordinate of Axis Origin	0
Angular velocity	0
Temperature	303
Turbulence Specification Method	0
Turb. Kinetic Energy	1
Turb. Dissipation Rate	1
Turbulence Intensity	0.1
Turbulence Length Scale	1
Hydraulic Diameter	1
Turbulent Viscosity Ratio	10
is zone used in mixing-plane model?	no

plates

Condition	Value
Wall Thickness	0.003
Heat Generation Rate	0
Material Name	perspex
Thermal BC Type	3
Temperature	300
Heat Flux	0
Convective Heat Transfer Coefficient	0
Free Stream Temperature	300
Wall Motion	0
Shear Boundary Condition	0
Define wall motion relative to adjacent cell zone?	yes
Apply a rotational velocity to this wall?	no
Velocity Magnitude	0
X-Component of Wall Translation	1

Y-Component of Wall Translation	0
External Emissivity	1
External Radiation Temperature	300
Wall Roughness Height	0
Wall Roughness Constant	0.5
Rotation Speed	0
X-Position of Rotation-Axis Origin	0
Y-Position of Rotation-Axis Origin	0
X-component of shear stress	0
Y-component of shear stress	0
Surface tension gradient	0
Specularity Coefficient	0

aluminum

Condition	Value
Loss-Coefficient	3
Heat-Transfer-Coefficient	25
Temperature	343
Heat Flux	0

outlet

Condition	Value
Gauge Pressure	0
Backflow Total Temperature	301.70001
Backflow Direction Specification Method	1
X-Component of Flow Direction	1
Y-Component of Flow Direction	0
X-Component of Axis Direction	1
Y-Component of Axis Direction	0
Z-Component of Axis Direction	0
X-Coordinate of Axis Origin	0
Y-Coordinate of Axis Origin	0
Z-Coordinate of Axis Origin	0
Turbulence Specification Method	0
Backflow Turb. Kinetic Energy	1
Backflow Turb. Dissipation Rate	1
Backflow Turbulence Intensity	0.1

Backflow Turbulence Length Scale	1
Backflow Hydraulic Diameter	1
Backflow Turbulent Viscosity Ratio	10
is zone used in mixing-plane model?	no
Specify targeted mass-flow rate	no
Targeted mass-flow	1

wall_plastic

Condition	Value
Wall Thickness	0.003
Heat Generation Rate	0
Material Name	pvc
Thermal BC Type	2
Temperature	300
Heat Flux	0
Convective Heat Transfer Coefficient	1.1
Free Stream Temperature	301.70001
Wall Motion	0
Shear Boundary Condition	0
Define wall motion relative to adjacent cell zone?	yes
Apply a rotational velocity to this wall?	no
Velocity Magnitude	0
X-Component of Wall Translation	1
Y-Component of Wall Translation	0
Define wall velocity components?	no
X-Component of Wall Translation	0
Y-Component of Wall Translation	0
External Emissivity	1
External Radiation Temperature	300
Wall Roughness Height	0
Wall Roughness Constant	0.5
Rotation Speed	0
X-Position of Rotation-Axis Origin	0
Y-Position of Rotation-Axis Origin	0
X-component of shear stress	0
Y-component of shear stress	0
Surface tension gradient	0
Specularity Coefficient	0

velocity_inlet

Condition	Value
Velocity Specification Method	2
Reference Frame	0
Velocity Magnitude	0.0094710002
X-Velocity	0
Y-Velocity	0
X-Component of Flow Direction	1
Y-Component of Flow Direction	0
X-Component of Axis Direction	1
Y-Component of Axis Direction	0
Z-Component of Axis Direction	0
X-Coordinate of Axis Origin	0
Y-Coordinate of Axis Origin	0
Z-Coordinate of Axis Origin	0
Angular velocity	0
Temperature	303
Turbulence Specification Method	0
Turb. Kinetic Energy	1
Turb. Dissipation Rate	1
Turbulence Intensity	0.1
Turbulence Length Scale	1
Hydraulic Diameter	1
Turbulent Viscosity Ratio	10
is zone used in mixing-plane model?	no

```
default-interior

   Condition   Value
   -----------------

plates:001

   Condition                                                 Value
   ----------------------------------------------------------------
   Wall Thickness                                            0
   Heat Generation Rate                                      0
   Material Name                                             perspex
   Thermal BC Type                                           1
   Temperature                                               300
   Heat Flux                                                 0
   Convective Heat Transfer Coefficient                      0
   Free Stream Temperature                                   300
   Wall Motion                                               0
   Shear Boundary Condition                                  0
   Define wall motion relative to adjacent cell zone?        yes
   Apply a rotational velocity to this wall?                 no
   Velocity Magnitude                                        0
   X-Component of Wall Translation                           1
   Y-Component of Wall Translation                           0
   Define wall velocity components?                          no
   X-Component of Wall Translation                           0
   Y-Component of Wall Translation                           0
   External Emissivity                                       1
   External Radiation Temperature                            300
   Wall Roughness Height                                     0
   Wall Roughness Constant                                   0.5
   Rotation Speed                                            0
   X-Position of Rotation-Axis Origin                        0
   Y-Position of Rotation-Axis Origin                        0
   X-component of shear stress                               0
   Y-component of shear stress                               0
   Surface tension gradient                                  0
   Specularity Coefficient                                   0
```

APPENDIX G

Material Properties

Material: pvc (solid)

Property	Units	Method	Value(s)
Density	kg/m3	constant	1390
Cp (Specific Heat)	j/kg-k	constant	900
Thermal Conductivity	w/m-k	constant	0.19

Material: perspex (solid)

Property	Units	Method	Value(s)
Density	kg/m3	constant	1150
Cp (Specific Heat)	j/kg-k	constant	1450
Thermal Conductivity	w/m-k	constant	0.25

Material: air (fluid)

Property	Units	Method	Value(s)
Density	kg/m3	constant	1.225
Cp (Specific Heat)	j/kg-k	constant	1006.43
Thermal Conductivity	w/m-k	constant	0.0242
Viscosity	kg/m-s	constant	1.7894001e-05
Molecular Weight	kg/kgmol	constant	28.966
L-J Characteristic Length	angstrom	constant	3.711
L-J Energy Parameter	k	constant	78.6
Thermal Expansion Coefficient	1/k	constant	0
Degrees of Freedom		constant	0
Speed of Sound	m/s	none	#f

Material: aluminum (solid)

Property	Units	Method	Value(s)
Density	kg/m3	constant	2719
Cp (Specific Heat)	j/kg-k	constant	871
Thermal Conductivity	w/m-k	constant	202.39999

APPENDIX H

```
Boundary Conditions
-------------------

   Zones

      name                id   type
      ---------------------------------------
      fluid               2    fluid
      aluminum-shadow     14   wall
      aluminum            7    wall
      trays:001-shadow    13   wall
      wall                3    wall
      velocity_inlet3     4    velocity-inlet
      vin2                5    velocity-inlet
      trays               6    wall
      outlet              8    pressure-outlet
      wall_plastic        9    wall
      velocity_inlet      10   velocity-inlet
      default-interior    12   interior
      trays:001           1    wall

   Boundary Conditions

      fluid

         Condition                                                  Value
         ------------------------------------------------------------------
         Material Name                                              air
         Specify source terms?                                      no
         Source Terms                                               ()
         Specify fixed values?                                      no
         Fixed Values                                               ()
         Motion Type                                                0
         X-Velocity Of Zone                                         0
         Y-Velocity Of Zone                                         0
         Rotation speed                                             0
         X-Origin of Rotation-Axis                                  0
         Y-Origin of Rotation-Axis                                  0
         Deactivated Thread                                         no
         Laminar zone?                                              no
         Set Turbulent Viscosity to zero within laminar zone?       no
```

Porous zone?	no
X-Component of Direction-1 Vector	1
Y-Component of Direction-1 Vector	0
Direction-1 Viscous Resistance	0
Direction-2 Viscous Resistance	0
Direction-1 Inertial Resistance	0
Direction-2 Inertial Resistance	0
C0 Coefficient for Power-Law	0
C1 Coefficient for Power-Law	0
Porosity	1
Solid Material Name	aluminum

aluminum-shadow

Condition	Value
Wall Thickness	0.0050000004
Heat Generation Rate	0
Material Name	aluminum
Thermal BC Type	3
Temperature	300
Heat Flux	0
Convective Heat Transfer Coefficient	0
Free Stream Temperature	300
Wall Motion	0
Shear Boundary Condition	0
Define wall motion relative to adjacent cell zone?	yes
Apply a rotational velocity to this wall?	no
Velocity Magnitude	0
X-Component of Wall Translation	1
Y-Component of Wall Translation	0
Define wall velocity components?	no
X-Component of Wall Translation	0
Y-Component of Wall Translation	0
External Emissivity	1
External Radiation Temperature	300
Wall Roughness Height	0
Wall Roughness Constant	0.5
Rotation Speed	0
X-Position of Rotation-Axis Origin	0
Y-Position of Rotation-Axis Origin	0
X-component of shear stress	0

Y-component of shear stress	0
Surface tension gradient	0
Specularity Coefficient	0

aluminum

Condition	Value
Wall Thickness	0.0050000004
Heat Generation Rate	0
Material Name	aluminum
Thermal BC Type	3
Temperature	300
Heat Flux	0
Convective Heat Transfer Coefficient	0
Free Stream Temperature	300
Wall Motion	0
Shear Boundary Condition	0
Define wall motion relative to adjacent cell zone?	yes
Apply a rotational velocity to this wall?	no
Velocity Magnitude	0
X-Component of Wall Translation	1
Y-Component of Wall Translation	0
Define wall velocity components?	no
X-Component of Wall Translation	0
Y-Component of Wall Translation	0
External Emissivity	1
External Radiation Temperature	300
Wall Roughness Height	0
Wall Roughness Constant	0.5
Rotation Speed	0
X-Position of Rotation-Axis Origin	0
Y-Position of Rotation-Axis Origin	0
X-component of shear stress	0
Y-component of shear stress	0
Surface tension gradient	0
Specularity Coefficient	0

trays:001-shadow

Condition	Value
Wall Thickness	0.003
Heat Generation Rate	0
Material Name	perspex
Thermal BC Type	3
Temperature	300
Heat Flux	0
Convective Heat Transfer Coefficient	0
Free Stream Temperature	300
Wall Motion	0
Shear Boundary Condition	0
Define wall motion relative to adjacent cell zone?	yes
Apply a rotational velocity to this wall?	no
Velocity Magnitude	0
X-Component of Wall Translation	1
Y-Component of Wall Translation	0
Define wall velocity components?	no
X-Component of Wall Translation	0
Y-Component of Wall Translation	0
External Emissivity	1
External Radiation Temperature	300
Wall Roughness Height	0
Wall Roughness Constant	0.5
Rotation Speed	0
X-Position of Rotation-Axis Origin	0
Y-Position of Rotation-Axis Origin	0
X-component of shear stress	0
Y-component of shear stress	0
Surface tension gradient	0
Specularity Coefficient	0

wall

Condition	Value
Wall Thickness	0.003
Heat Generation Rate	0
Material Name	perspex
Thermal BC Type	2
Temperature	300
Heat Flux	0

Convective Heat Transfer Coefficient	6
Free Stream Temperature	303
Wall Motion	0
Shear Boundary Condition	0
Define wall motion relative to adjacent cell zone?	yes
Apply a rotational velocity to this wall?	no
Velocity Magnitude	0
X-Component of Wall Translation	1
Y-Component of Wall Translation	0
Define wall velocity components?	no
X-Component of Wall Translation	0
Y-Component of Wall Translation	0
External Emissivity	1
External Radiation Temperature	300
Wall Roughness Height	0
Wall Roughness Constant	0.5
Rotation Speed	0
X-Position of Rotation-Axis Origin	0
Y-Position of Rotation-Axis Origin	0
X-component of shear stress	0
Y-component of shear stress	0
Surface tension gradient	0
Specularity Coefficient	0

velocity_inlet3

Condition	Value
Velocity Specification Method	2
Reference Frame	0
Velocity Magnitude	0.5
X-Velocity	0
Y-Velocity	0
X-Component of Flow Direction	1
Y-Component of Flow Direction	0
X-Component of Axis Direction	1
Y-Component of Axis Direction	0
Z-Component of Axis Direction	0
X-Coordinate of Axis Origin	0
Y-Coordinate of Axis Origin	0
Z-Coordinate of Axis Origin	0

Z-Coordinate of Axis Origin	0
Angular velocity	0
Temperature	328
Turbulence Specification Method	0
Turb. Kinetic Energy	1
Turb. Dissipation Rate	1
Turbulence Intensity	0.1
Turbulence Length Scale	1
Hydraulic Diameter	1
Turbulent Viscosity Ratio	10
is zone used in mixing-plane model?	no

vin2

Condition	Value
Velocity Specification Method	2
Reference Frame	0
Velocity Magnitude	0.00079999998
X-Velocity	0
Y-Velocity	0
X-Component of Flow Direction	1
Y-Component of Flow Direction	0
X-Component of Axis Direction	1
Y-Component of Axis Direction	0
Z-Component of Axis Direction	0
X-Coordinate of Axis Origin	0
Y-Coordinate of Axis Origin	0
Z-Coordinate of Axis Origin	0
Angular velocity	0
Temperature	303
Turbulence Specification Method	0
Turb. Kinetic Energy	1
Turb. Dissipation Rate	1
Turbulence Intensity	0.1
Turbulence Length Scale	1
Hydraulic Diameter	1
Turbulent Viscosity Ratio	10
is zone used in mixing-plane model?	no

trays

Condition	Value
Wall Thickness	0.003
Heat Generation Rate	0
Material Name	perspex
Thermal BC Type	1
Temperature	300
Heat Flux	0
Convective Heat Transfer Coefficient	0
Free Stream Temperature	300
Wall Motion	0
Shear Boundary Condition	0
Define wall motion relative to adjacent cell zone?	yes
Apply a rotational velocity to this wall?	no
Velocity Magnitude	0
X-Component of Wall Translation	1
Y-Component of Wall Translation	0
Define wall velocity components?	no
X-Component of Wall Translation	0
Y-Component of Wall Translation	0
External Emissivity	1
External Radiation Temperature	300
Wall Roughness Height	0
Wall Roughness Constant	0.5
Rotation Speed	0
X-Position of Rotation-Axis Origin	0
Y-Position of Rotation-Axis Origin	0
X-component of shear stress	0
Y-component of shear stress	0
Surface tension gradient	0
Specularity Coefficient	0

outlet

Condition	Value
Gauge Pressure	0
Backflow Total Temperature	300
Backflow Direction Specification Method	1

X-Component of Flow Direction	1
Y-Component of Flow Direction	0
X-Component of Axis Direction	1
Y-Component of Axis Direction	0
Z-Component of Axis Direction	0
X-Coordinate of Axis Origin	0
Y-Coordinate of Axis Origin	0
Z-Coordinate of Axis Origin	0
Turbulence Specification Method	0
Backflow Turb. Kinetic Energy	1
Backflow Turb. Dissipation Rate	1
Backflow Turbulence Intensity	0.1
Backflow Turbulence Length Scale	1
Backflow Hydraulic Diameter	1
Backflow Turbulent Viscosity Ratio	10
is zone used in mixing-plane model?	no
Specify targeted mass-flow rate	no
Targeted mass-flow	1

wall_plastic

Condition	Value
Wall Thickness	0.003
Heat Generation Rate	0
Material Name	pvc
Thermal BC Type	2
Temperature	300
Heat Flux	0
Convective Heat Transfer Coefficient	1.1
Free Stream Temperature	303
Wall Motion	0
Shear Boundary Condition	0
Define wall motion relative to adjacent cell zone?	yes
Apply a rotational velocity to this wall?	no
Velocity Magnitude	0
X-Component of Wall Translation	1
Y-Component of Wall Translation	0
Define wall velocity components?	no
X-Component of Wall Translation	0
Y-Component of Wall Translation	0

External Emissivity	1
External Radiation Temperature	300
Wall Roughness Height	0
Wall Roughness Constant	0.5
Rotation Speed	0
X-Position of Rotation-Axis Origin	0
Y-Position of Rotation-Axis Origin	0
X-component of shear stress	0
Y-component of shear stress	0
Surface tension gradient	0
Specularity Coefficient	0

velocity_inlet

Condition	Value
Velocity Specification Method	2
Reference Frame	0
Velocity Magnitude	0.000459
X-Velocity	0
Y-Velocity	0
X-Component of Flow Direction	1
Y-Component of Flow Direction	0
X-Component of Axis Direction	1
Y-Component of Axis Direction	0
Z-Component of Axis Direction	0
X-Coordinate of Axis Origin	0
Y-Coordinate of Axis Origin	0
Z-Coordinate of Axis Origin	0
Angular velocity	0
Temperature	303
Turbulence Specification Method	0
Turb. Kinetic Energy	1
Turb. Dissipation Rate	1
Turbulence Intensity	0.1
Turbulence Length Scale	1
Hydraulic Diameter	1
Turbulent Viscosity Ratio	10
is zone used in mixing-plane model?	no

default-interior

Condition	Value

trays:001

Condition	Value
Wall Thickness	0.003
Heat Generation Rate	0
Material Name	perspex
Thermal BC Type	3
Temperature	300
Heat Flux	0
Convective Heat Transfer Coefficient	0
Free Stream Temperature	300
Wall Motion	0
Shear Boundary Condition	0
Define wall motion relative to adjacent cell zone?	yes
Apply a rotational velocity to this wall?	no
Velocity Magnitude	0
X-Component of Wall Translation	1
Y-Component of Wall Translation	0
Define wall velocity components?	no
X-Component of Wall Translation	0
Y-Component of Wall Translation	0
External Emissivity	1
External Radiation Temperature	300
Wall Roughness Height	0
Wall Roughness Constant	0.5
Rotation Speed	0
X-Position of Rotation-Axis Origin	0
Y-Position of Rotation-Axis Origin	0
X-component of shear stress	0
Y-component of shear stress	0
Surface tension gradient	0
Specularity Coefficient	0

APPENDIX I

Simulation Data for Scenario 1 (Solar Energy)

Time (24 hours)	**$T_{inlet/ambient}$ (K)**	**$T_{near\ absorber}$ (K)**	**$T_{absorber}$ (K)**	**$T_{chamber}$ (K)**	**T_{outlet} (K)**	**$V_{in\ 1}$ (m/s)**	**$V_{in\ 2}$ (m/s)**	**$V_{chimney}$ (m/s)**
900	301.7	314.20859	343	307.45016	305.28575	0.009470	0.0008	0.20479
1000	303.1	313.64862	346	309.12445	306.86237	0.011271	0.0008	0.24393
1100	303.0	315.45724	354	310.11481	307.44357	0.012171	0.0008	0.26344
1200	304.2	319.32290	358	310.66360	310.66360	0.011721	0.0008	0.25365
1300	303.9	316.14310	356	310.39954	310.39954	0.014422	0.0008	0.31189
1400	303.5	315.91700	354	310.59170	307.92886	0.011271	0.0008	0.24390
1500	303.5	315.03827	347	309.57886	309.57886	0.010821	0.0008	0.23410
1600	303.1	312.15920	343	307.93845	307.93845	0.008570	0.0008	0.18600
1700	302.8	312.23199	337	306.91025	306.91025	0.008120	0.0008	0.17564

APPENDIX J

Simulation Data for Scenario 2 (Biomass Energy)

Time (24 hours)	**$T_{inlet\ /\ biomass\ burner}$ (K)**	**$T_{near\ absorber}$ (K)**	**$T_{absorber}$ (K)**	**$T_{chamber}$ (K)**	**T_{outlet} (K)**	**$V_{in\ 1}$ (m/s)**	**$V_{in\ 2}$ (m/s)**	**$V_{in\ 3\ /\ biomass\ burner}$ (m/s)**	**$V_{chimney}$ (m/s)**
1545	330.0	321.872	327.361	324.080	316.383	0.004965	0.0008	0.250	0.490
1600	328.0	321.821	326.840	319.312	318.057	0.005415	0.0008	0.240	0.384
1615	327.8	320.426	325.405	319.181	317.937	0.005415	0.0008	0.240	0.384
1630	327.7	320.356	325.315	319.116	317.876	0.005415	0.0008	0.240	0.384
1645	327.2	320.005	324.863	318.790	317.575	0.005415	0.0008	0.240	0.384
1700	326.4	319.441	321.790	318.267	317.093	0.004740	0.0008	0.235	0.374
1715	318.9	314.171	317.362	312.575	312.575	0.005866	0.0008	0.220	0.354
1730	313.0	310.008	312.025	308.990	308.496	0.006541	0.0008	0.215	0.381
1745	313.0	310.002	312.531	309.019	308.517	0.006091	0.0008	0.215	0.381

APPENDIX K

Experimental Data for Scenario 1 (Solar Energy)

Time (24 hours)	**$T_{inlet/ambient}$ (K)**	**$T_{near\ absorber}$ (K)**	**$T_{absorber}$ (K)**	**$T_{chamber}$ (K)**	**T_{outlet} (K)**	**$V_{chimney}$ (m/s)**
900	301.7	317.5	343	315.2	304.9	0.22
1000	303.1	320.3	346	318.6	306.1	0.26
1100	303.0	328.6	354	323.2	308.1	0.28
1200	304.2	336.1	358	328.9	311.1	0.27
1300	303.9	329.1	356	330.0	310.8	0.33
1400	303.5	328.8	354	326.4	310.1	0.26
1500	303.5	327.4	347	323.5	308.9	0.25
1600	303.1	320.4	343	319.1	305.1	0.20
1700	302.8	316.2	337	313.8	304.3	0.19

APPENDIX L

Experimental Data for Scenario 2 (Flue Gas)

Time (24 hours)	**$T_{absorber}$ (K)**	**$T_{near\ absorber}$ (K)**	**$Humidity_{near\ absorber}$ (%)**	**$T_{chamber}$ (K)**	**$Humidity_{chamber}$(%)**	**$T_{wet\ bulb\ @\ inlet}$ (K)**	**$T_{dry\ bulb\ @\ inlet}$ (K)**	**$T_{wet\ bulb\ @\ outlet}$ (K)**	**$T_{dry\ bulb\ @\ outlet}$ (K)**	**T_{outlet} (K)**	**$V_{chimney}$ (m/s)**
1545	328.0	320.4	46.8	316.1	66.5	312.2	309.1	304.9	301.8	310.0	0.50
1600	326.0	314.1	45.3	313.6	71.6	312.0	308.9	304.8	301.6	309.0	0.40
1615	325.8	314.9	65.6	313.8	75.4	311.4	308.9	304.1	300.5	308.6	0.39
1630	325.7	314.8	64.7	313.8	83.8	311.7	300.7	303.7	300.5	308.5	0.39
1645	325.2	315.3	54.1	312.9	71.2	306.3	303.8	303.5	299.6	308.5	0.38
1700	324.4	314.7	58.3	312.1	77.2	307.2	304.8	303.1	300.1	308.8	0.35
1715	316.9	311.9	62.9	309.7	74.1	305.4	304.5	301.5	299.4	306.5	0.36
1730	315.0	311.2	60.1	309.0	69.2	304.8	301.5	301.4	298.8	306.3	0.37
1745	315.0	310.3	64.6	307.8	72.5	304.2	301.3	301.3	298.9	305.5	0.36

APPENDIX M

Experimental Data for Scenario 2 (Clean, warm air)

Time (24 hours)	**$T_{absorber}$ (K)**	**$T_{near\ absorber}$ (K)**	**$Humidity_{near\ absorber}$ (%)**	**$T_{chamber}$ (K)**	**$Humidity_{chamber}$(%)**	**$T_{wet\ bulb\ @\ inlet}$ (K)**	**$T_{dry\ bulb\ @\ inlet}$ (K)**	**$T_{wet\ bulb\ @\ outlet}$ (K)**	**$T_{dry\ bulb\ @\ outlet}$ (K)**	**T_{outlet} (K)**	**$V_{chimney}$ (m/s)**
1815	311.0	308.7	67.0	305.9	70.6	301.3	298.4	300.0	298.3	305.0	0.40
1830	307.0	305.4	69.1	304.1	72.0	301.2	300.8	299.6	298.1	304.9	0.39
1845	306.5	305.4	71.4	304.0	83.7	300.7	299.1	300.0	298.1	304.6	0.38
1900	306.6	305.2	71.9	303.8	84.9	300.8	299.3	300.1	298.6	304.9	0.39
1915	304.8	303.8	83.9	303.0	89.4	300.6	299.5	300.1	298.9	303.6	0.37

APPENDIX N

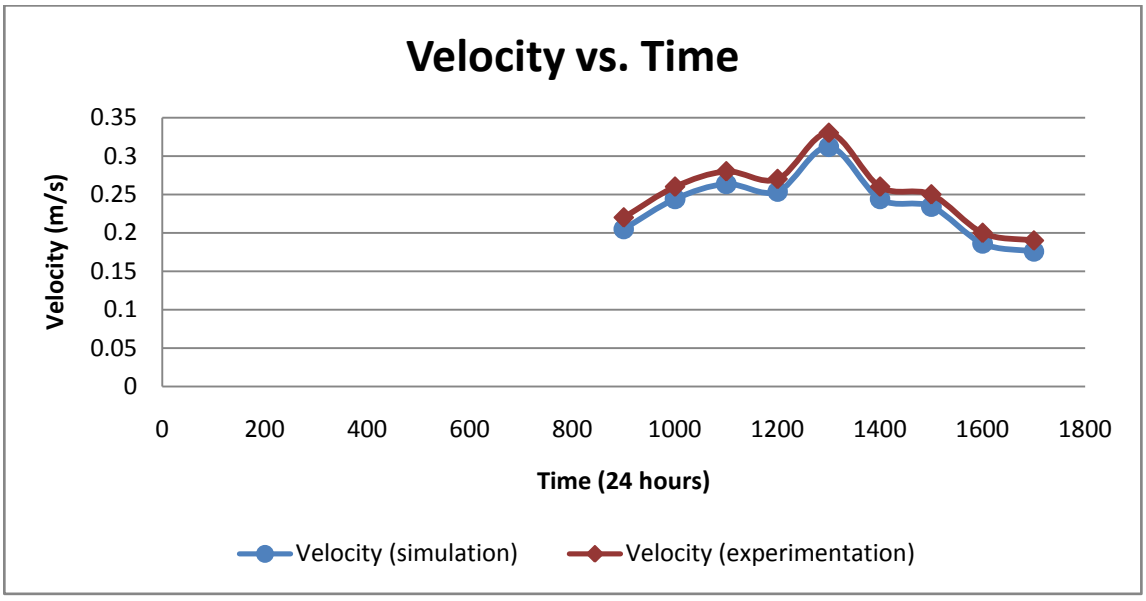

Comparison of velocity outlet for simulation and experimental model for Scenario 1 (Solar Energy)

APPENDIX O

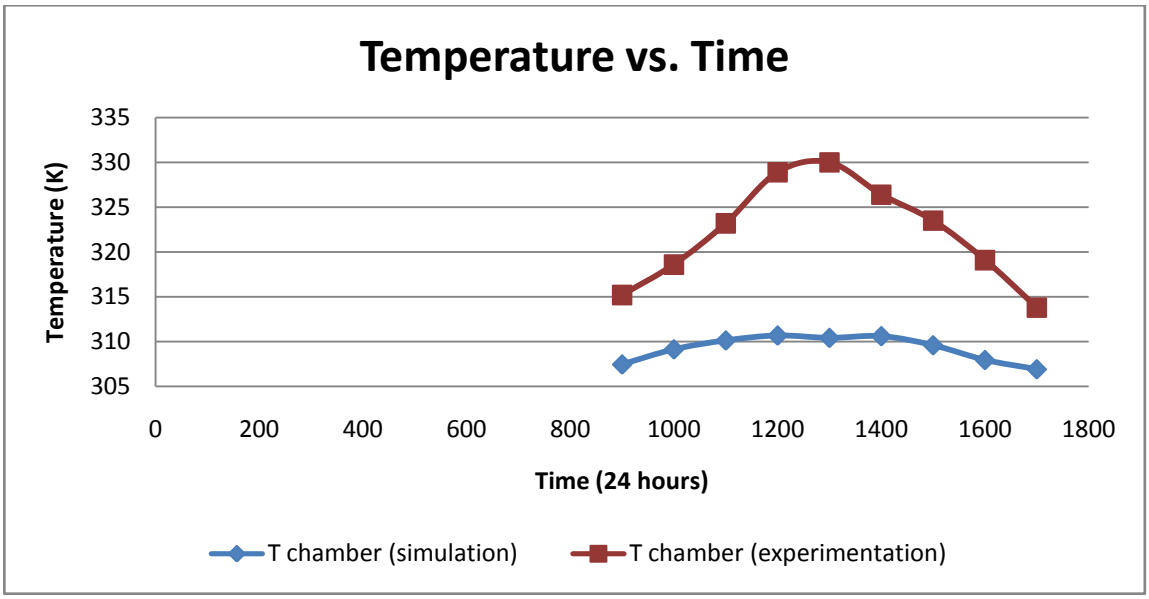

Comparison of temperature in chamber for simulation and experimental data for Scenario 1 (Solar Energy)

APPENDIX P

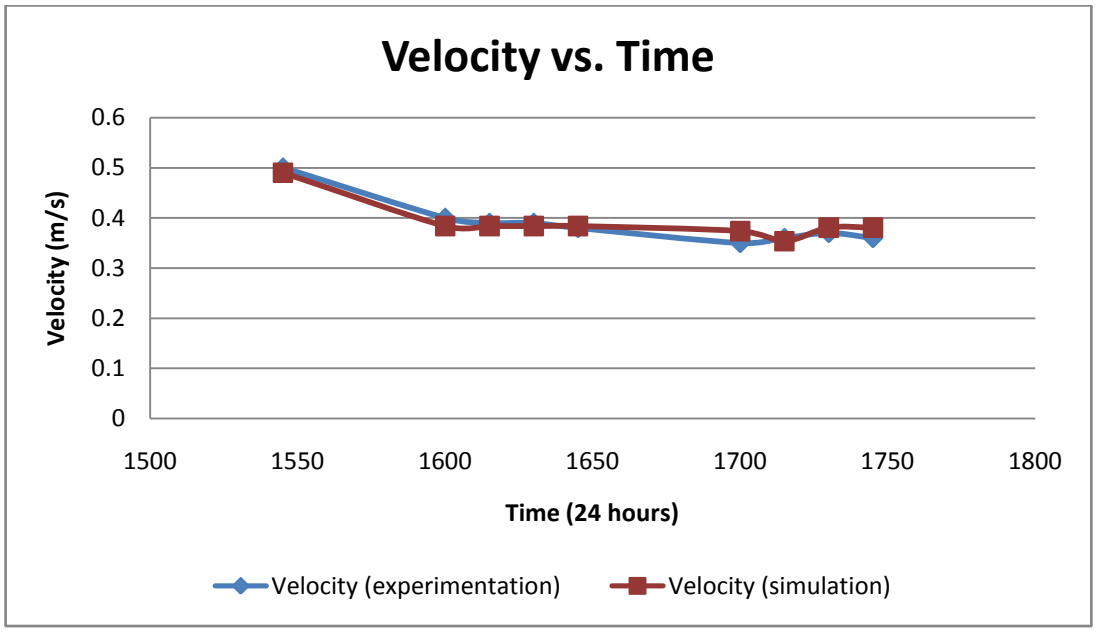

Comparison of velocity outlet for simulation and experimental model for Scenario 2 (Biomass Energy)

APPENDIX Q

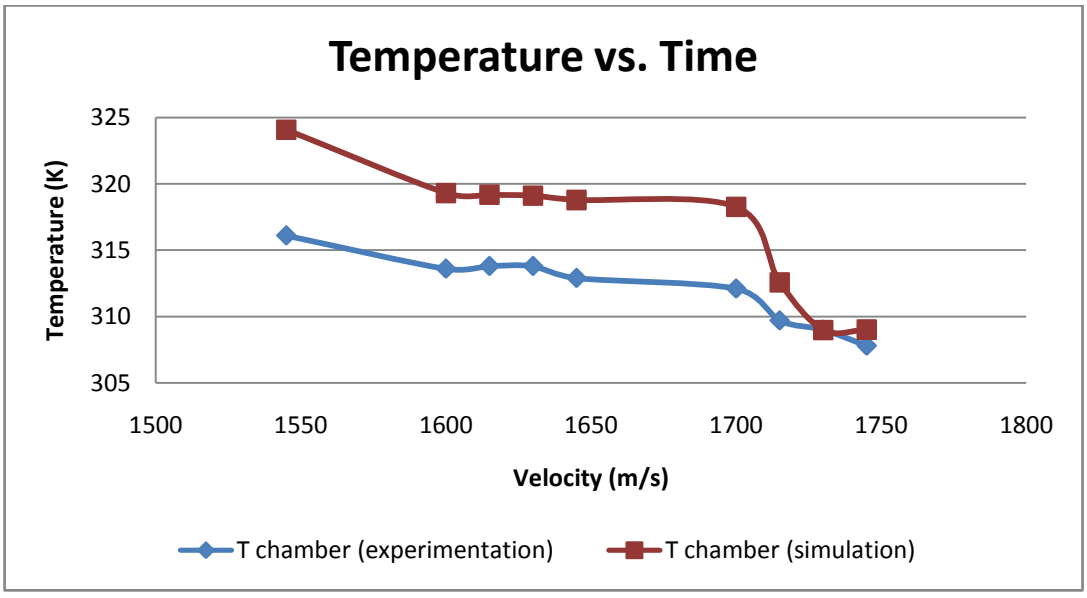

Comparison of temperature in chamber for simulation and experimental data for Scenario 2 (Biomass Energy)